

HOLOCENE COASTAL CHANGES ALONG THE GIRONDE ESTUARY (SW FRANCE): NEW INSIGHTS FROM THE NORTH MÉDOC PENINSULA BEACH/DUNE SYSTEM

Pierre STÉPHAN¹, Florence VERDIN², Gilles ARNAUD-FASSETTA³, Frédéric BERTRAND³, Frédérique EYNAUD⁴, Ane GARCÍA-ARTOLA⁵, Mathieu BOSQ⁶, Camille CULIOLI³, Serge SUANEZ¹, Clément COUTELIER², Pascal BERTRAN^{6,7} & Stéphane COSTA¹

ABSTRACT

L'Amélie beach is located near the mouth of the Gironde estuary (south-western Atlantic coast of France). It has been greatly eroded by recent storms, especially in the winter of 2013-2014. Erosion of the dune front and beach has uncovered a set of estuarine and aeolian sediment deposits containing numerous archaeological remains. A campaign of topographic surveys was undertaken with DGPS and TLS equipment during the springs of 2014 and 2015 along the 2 km length of L'Amélie beach in order to reconstruct the elevation and stratigraphy of these deposits. Sedimentological analyses (grain size, micro-faunal) were performed to better constrain the depositional environment. Archaeological remains and several radiocarbon dates obtained from sediment samples collected in the field were used to propose a consistent chronological framework for this sedimentary sequence. Ten main lithofacies were distinguished from the lower part of the beach to the top of the dune. The base of the sedimentary sequence is composed of Pleistocene deposits dating from MIS 9 (unit 1a) to MIS 2 (unit 1b) (Bosq *et al.*, 2019). The Holocene sedimentary infilling began around 5000 BC with an accumulation of coarse marine sands, which suggests the presence of a tidal inlet. On both sides of this tidal channel, archaeological remains dating from the early Neolithic period up to the Bronze Age testify to a human occupation of the coastal area. From ca. 5000 to ca. 3500 cal. a BP, a characteristic deposit of intertidal mudflats indicates the transformation of the tidal inlet into estuarine marshes protected by a coastal dune barrier. Between ca. 3500 and ca. 3000 cal. a BP, the dune barrier records a phase of erosion resulting in the exposure of the marsh to stronger hydrodynamic conditions. From ca. 2800 to 1650 cal. a BP, a second phase of estuarine sedimentation is recognized. This period is characterized by significant human occupation as indicated by the presence of numerous archaeological remains of the Iron Age and Gallo-Roman periods, associated with the exploitation of a saltwater-to-brackish environment. From 1650 to 1250 cal. a BP, the estuarine salt marsh is gradually overrun by northward migrating coastal-dune fields. After 1250 cal. a BP, the marsh is completely covered by aeolian sands. These results are consistent with previously published data and allow us to detail the local sequence of palaeogeographic changes of the north-Médoc peninsula. Using the 'sea-level index points' method (Hijma *et al.*, 2015), the analysis of radiocarbon dated levels also provides new relative sea level records for this part of the French Atlantic coast. Finally, the phases of coastal dune activity/stability recognized along L'Amélie beach are synchronous with those in the wider Aquitaine coastal region, suggesting a regional driving factor. We propose that the shared sedimentary dynamics are the consequence of the onshore migration of intertidal and subtidal sand banks distributed at the mouth of the Gironde.

Keywords: Holocene, estuary, dune, mudflat, salt marsh, sea-level rise, aeolian sand drift, TLS, Gironde, Aquitaine

RÉSUMÉ

CHANGEMENTS CÔTIERS HOLOCÈNES LE LONG DE L'ESTUAIRE DE LA GIRONDE : NOUVELLES DONNÉES À PARTIR DU SYSTÈME PLAGE/DUNE DE LA PÉNINSULE DU NORD-MÉDOC

Le long du littoral de Soulac, à l'embouchure de la Gironde, l'érosion marine provoquée par les récentes tempêtes hivernales a mis au jour un ensemble de dépôts sédimentaires à caractère estuaire et dunaire contenant de nombreux vestiges archéologiques. Des relevés topographiques réalisés au DGPS et TLS durant les printemps 2014 et 2015 ont été effectués le long des 2 km de la plage de l'Amélie dans le but de reconstruire la stratigraphie de ces dépôts. Des analyses sédimentologiques (granulométrie, micro-faune) ont été réalisées afin de caractériser les unités lithologiques et reconstituer le cadre paléoenvironnemental. L'étude du mobilier archéologique et plusieurs datations par le radiocarbone ont permis de proposer un cadre chronologique cohérent pour cette séquence sédimentaire. Dix principaux lithofaciès ont été distingués depuis le bas de plage jusqu'au sommet de la dune. La base de la séquence se compose de formations pléistocènes datée du MIS 9 au MIS 2 (Bosq *et al.*, 2019), lesquelles montrent une topographie déprimée dans la partie centrale de la plage de l'Amélie. Le colmatage sédimentaire de cette dépression débute vers 5000 BC par le dépôt d'un sable grossier marin suggérant la présence d'une passe tidale. De part et d'autre de ce vaste chenal de marée, des vestiges archéologiques datant du Néolithique ancien jusqu'à l'âge du Bronze témoignent d'une occupation humaine du secteur. De 5000 à 3500 a cal. BP environ, un dépôt caractéristique des vasières intertidales indique la transformation du milieu en marais estuaire protégé par un cordon dunaire. Entre 3500 et 3000 a cal. BP, ce cordon enregistre une phase d'érosion qui se solde par l'ouverture du marais sur la mer. De 2800 à 1650 a cal. BP, une seconde phase de sédimentation estuaire est reconnue, signalant le retour à des conditions d'abri. Cette période se caractérise par une forte occupation humaine et la présence de nombreux vestiges archéologiques de l'âge du Fer et de l'Antiquité associés à l'exploitation d'un environnement intertidal à saumâtre. De 1650 à 1250 a cal. BP, le marais est progressivement colmaté par les dépôts dunaires qui progradent en direction du nord. Après 1250 a cal. BP, le marais est entièrement recouvert par les sables éoliens. Ces résultats sont cohérents avec les données publiées antérieurement et permettent de détailler localement la séquence des changements paléogéographiques de la péninsule du nord-médoc. En appliquant la méthode des « sea-level index points » (Hijma *et al.*, 2015), l'analyse des niveaux datés par le radiocarbone apporte également de nouvelles données sur la remontée du niveau marin relatif dans cette partie du littoral atlantique français. Enfin, les phases d'activité et de stabilité des dunes reconnues le long de la plage de l'Amélie montre un déphasage par rapport aux évolutions dunaires du reste de la côte aquitaine et suggère une dynamique sédimentaire influencée par la migration vers la côte des bancs de sables intertidaux et subtidaux distribués à l'embouchure de la Gironde.

Mots-clés : Holocene, estuary, dune, vasière, marais maritimes, hausse du niveau marin, ensablement éolien, TLS, Gironde, Aquitaine

1 - INTRODUCTION

During the Holocene period, most estuaries in the world recorded significant environmental and palaeogeographical changes in response to (1) transgression (induced by post-glacial sea-level rise) of irregular-shaped Pleistocene fluvial-incised valleys that controlled accommodation space, (2) changes in regional and global climate and human activities that affected sediment supply to the estuaries and, (3) tectonics (e.g. Fletcher *et al.*, 1990 ; Zaitlin *et al.*, 1994 ; Ruiz *et al.*, 2004 ; Boyd *et al.*, 2006 ; Anderson *et al.*, 2008 ; Chaumillon *et al.*, 2010 ; Schneider *et al.*, 2010 ;

Durand *et al.*, 2016 ; Clement *et al.*, 2017). Studies of the Holocene sedimentary fill of estuaries show that the nature and organization of facies within incised-valley estuaries was controlled by the interplay between marine processes (waves and tides), which generally decrease in intensity up-estuary, and fluvial processes, which decrease in strength down-estuary (Dalrymple *et al.*, 1992).

Located on the SW Atlantic coast of France, the Gironde is a tide-dominated estuary, with a 20 km wide tidal mouth open to the Atlantic Ocean (fig. 1) where wave and aeolian processes have led to the construction of coastal dune barriers that are affected by episodic storm-induced erosion. Seismic stratigraphic investigations

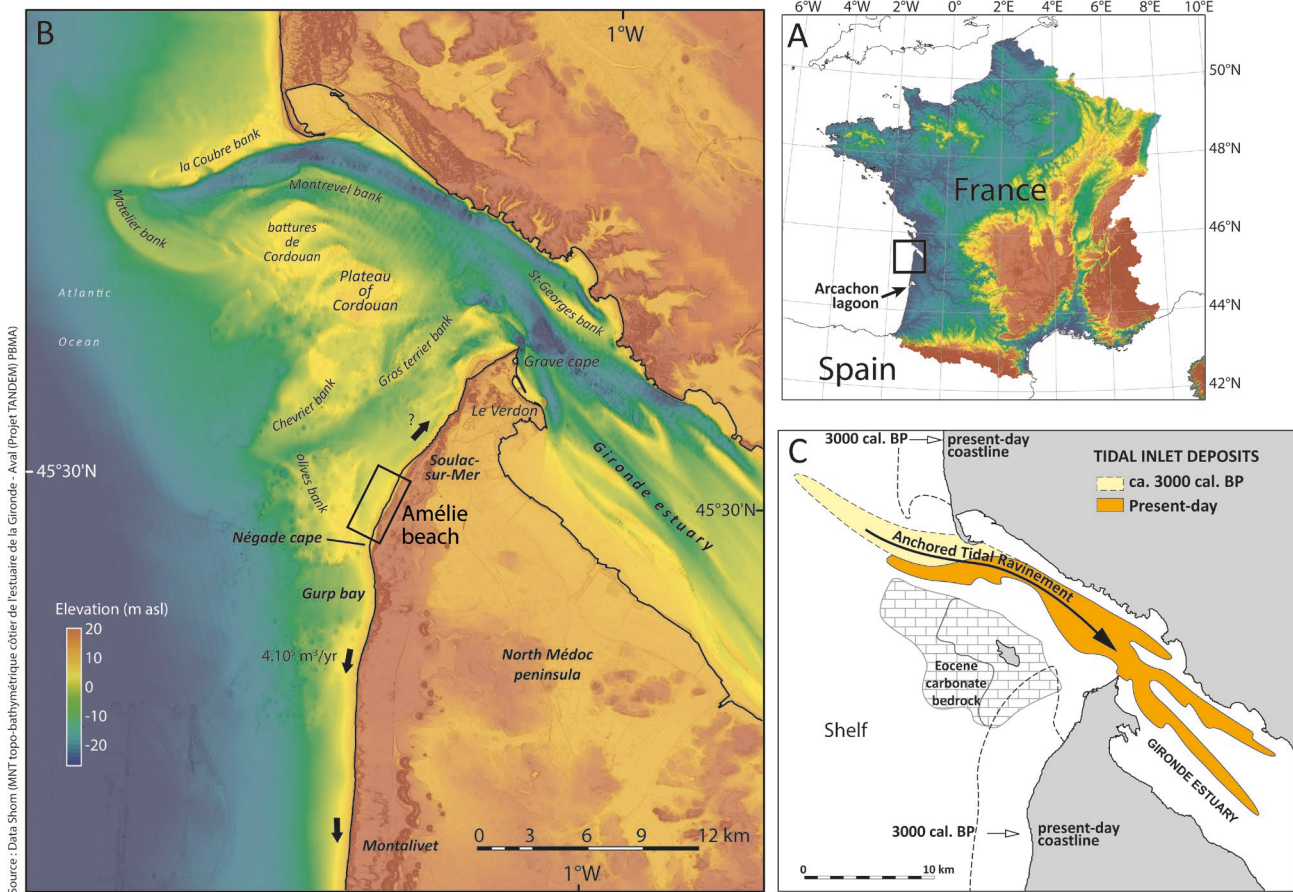


Fig. 1: Location maps of the study site.

(A) Location of the North Médoc peninsula and the Gironde estuary along the Atlantic coast of France. (B) Topo-bathymetric digital elevation model of the mouth of the Gironde estuary showing the numerous sandbanks in the intertidal and subtidal areas. Black arrows indicate the main direction of the longshore drift and the value corresponds to the volume of sediment transfer. (C) “Anchored tidal ravinement process” and associated ribbon-shaped reservoir geometry (from Feniès *et al.*, 2010).

*Fig. 1 : Cartes de localisation du secteur d'étude. (A) Localisation de la péninsule du Nord-Médoc et de l'embouchure de la Gironde le long des côtes atlantiques françaises. (B) Modèle numérique de terrain représentant la topo-bathymétrie et révélant les nombreux bancs sableux dans les zones intertidales et subtidales. Les flèches noires indiquent le sens de la dérive littorale et la valeur correspond au volume des transferts sédimentaires. (C) Le processus de « ravinement tidal ancré » et la géométrie de réservoir en ruban engendrée par ce processus (Feniès *et al.*, 2010).*

¹ Laboratoire LETG (UMR 6554 CNRS), Université de Bretagne occidentale, Institut Universitaire Européen de la Mer, Place Nicolas Copernic, FR-29280 PLOUZANÉ. Emails : pierre.stephan@univ-brest.fr, stephane.costa@unicaen.fr, serge.suanez@univ-brest.fr

² Laboratoire AUSONIUS (UMR 5607 CNRS), Université Bordeaux Montaigne, Maison de l'archéologie, 8, esplanade des Antilles, FR-33607 PESSIONAC. Email : clement.coutelier@u-bordeaux-montaigne.fr, florence.verdin@u-bordeaux-montaigne.fr

³ Laboratoire PRODIG (UMR 8586 CNRS), Université Paris-Sorbonne, Institut de Géographie, 191 rue Saint-Jacques, FR-75005 PARIS. Emails : gilles.arnaud-fassetta@univ-paris-diderot.fr, culioli.camille2@gmail.com, Frederic.Bertrand@paris-sorbonne.fr

⁴ Laboratoire EPOC (UMR 5805 CNRS), Université de Bordeaux, Allée Geoffroy Saint Hilaire, CS 50023, 33615 FR-PESSAC, France. Courriel : frederique.eyraud@u-bordeaux.fr

⁵ Departamento de Estratigrafía y Paleontología, Universidad del País Vasco UPV/EHU, ESP-BILBAO. Email : ane.garcia@ehu.eus

⁶ Laboratoire PACEA (UMR 5199 CNRS), Université de Bordeaux, Allée Geoffroy Saint Hilaire, CS 50023, 33615 FR-PESSAC. Emails : mathieu.bosq@gmail.com, pascal.bertran@inrap.fr

⁷ INRAP, 140 avenue du Maréchal Leclerc, FR-33130 BÈGLES

along the inner and outer parts of the Gironde estuary show a sequence comprising a diverse assemblage of lithofacies that can be grouped into three main systems tracts (lowstand, transgressive and highstand systems tracts, fig. 2) (Allen & Posamentier, 1993; Lericolais *et al.*, 1998; Fénies *et al.*, 2010). The lowstand systems tract comprises a continuous unit of fluvial gravel and coarse sand deposited in the thalweg of the incised valley during the periods of low eustatic sea-level stand. The transgressive systems tract comprises the bulk of the incised valley fill and forms a landward-thinning wedge of tidal-estuarine sands and muds deposited during the post-glacial marine transgression (before 7000 cal. a BP). In the estuary mouth, these deposits are replaced by a thick unit of coarse-grained, estuary-mouth tidal-inlet and tidal-delta sands. At the same time, the adjacent shorelines were starved of sediment and eroded by waves. The highstand systems tract, initiated at about 7000-6000 cal. a BP, comprises seaward-prograding, tide-dominated estuarine bayhead delta deposits that

have gradually filled the estuary since the late-Holocene stillstand (Allen, 1991; Allen and Posamentier, 1993; Fénies and Tastet, 1998; Chaumillon *et al.*, 2013).

Studies carried out in the southern coastal marshes of the Gironde estuary suggest that, as relative sea-level rose to the elevation of the relatively flat fluvial terraces, these areas were flooded rapidly, resulting in rapid expansions of swamps and salt marshes in lateral bay areas (Diot & Tastet, 1995; Pontee *et al.*, 1998; Diot *et al.*, 2001). The development of these coastal marshes was favoured by the presence of a large dune barrier elongated to the north, forming the north-Médoc peninsula. Although the Holocene evolution of Aquitaine dune complexes has been studied in detail by many authors (Marionnaud & Dubreuilh, 1972; Tastet, 1998; Clavé, 2001; Clarke *et al.* 1999, 2002), the construction phases of the north-Médoc dune barrier are poorly known. Furthermore, very little attempt has been made to correlate either marsh development -on the western bank of the Gironde estuary- or dune development - on the ocean side of the

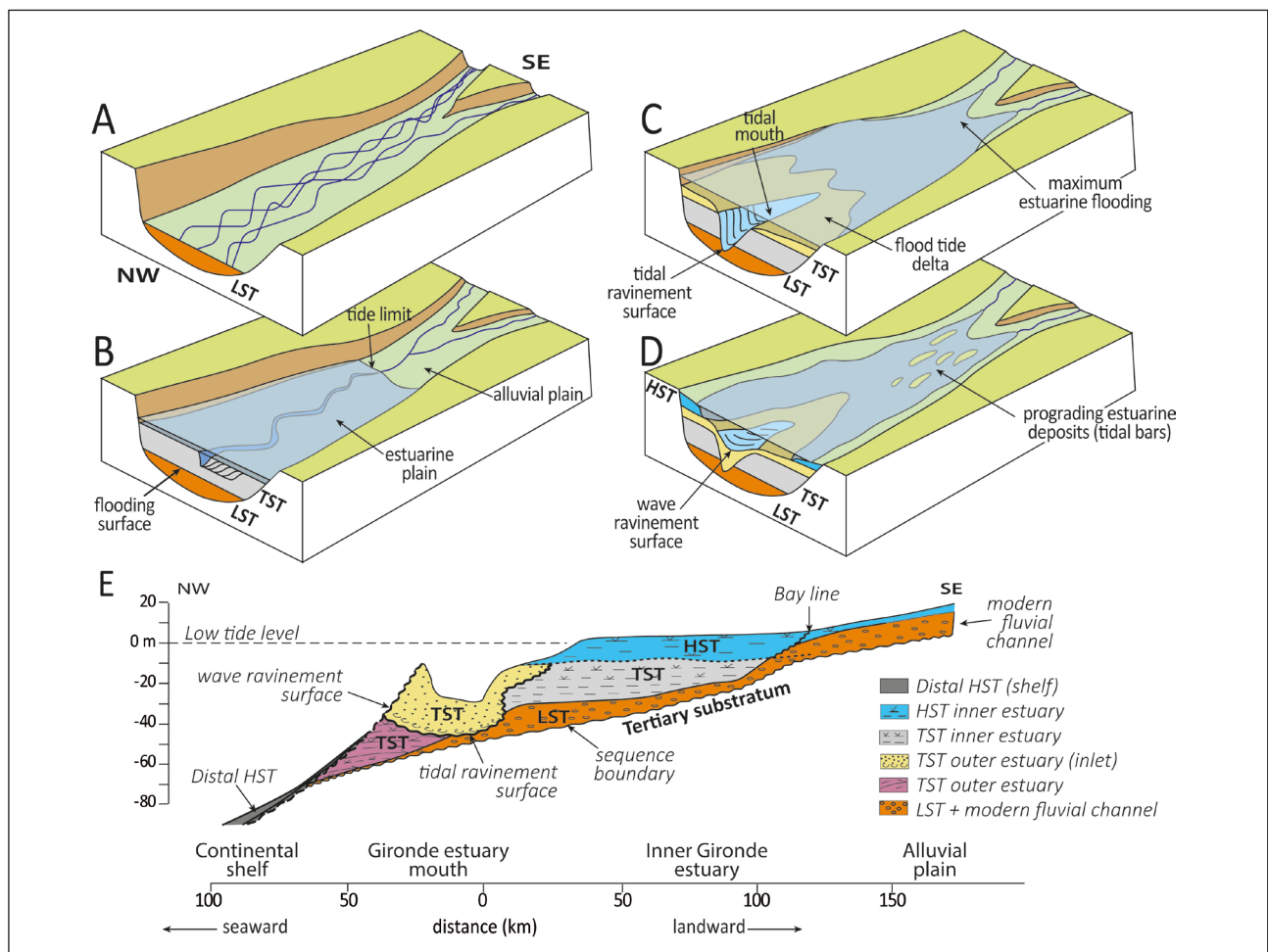


Fig. 2: Sequence of sedimentary fill of the Gironde estuary during the Holocene (modified from Lericolais *et al.* (2001), Fénies and Lericolais (2005) and Fénies *et al.* (2010)).

(A) Schematic illustration of the incised-valley of Gironde in the Early Holocene. (B) Schematic illustration of the initiation of post-glacial marine transgression into the valley. (C) Schematic illustration of the maximum marine flooding around 7000-6000 BP resulting in estuarine mud deposited in the funnel zone and landward migration of the tidal inlet. (D) Schematic illustration of the geological evolution of the Gironde estuary over the last 7000 years. A regressive tidal-estuarine bay-head delta has prograded into the upper estuary, gradually filling it with sediment. (E) Internal stratigraphy of the Gironde incised-valley fill.

*Fig. 2 : Séquence de remplissage sédimentaire de l'estuaire de la Gironde durant l'Holocène (modifié d'après Lericolais *et al.* (2001), Fénies et Lericolais (2005) et Fénies *et al.* (2010)). (A) La vallée incisée de la Gironde au début de l'Holocène. (B) Évolution géologique de l'estuaire lors de la transgression post-glaciaire. (C) Inondation maximale vers 7000-6000 BP, associée à un dépôt vaseux au niveau de l'estuaire amont et à une avancée de la passe de l'embouchure. (D) Période de haut niveau marin, relativement stable depuis 7000 ans, montrant la progradation d'un pro-delta estuarien formé de barres de marée, comblant progressivement l'estuaire. (E) Stratigraphie du remplissage de la vallée incisée de la Gironde.*

peninsula - with changes in configuration at the estuary mouth, notably in the vicinity of lateral bays which exhibited more or less wide openings onto the estuary and have yielded archaeological evidence of early human presence as around the 'Anse du Gürp', which is assumed to be a former mouth of the estuary.

During the winter of 2013-2014, significant erosion of the beaches and the dune front escarpment along the Aquitaine shoreline (Bulteau *et al.*, 2014; Castelle *et al.*, 2014, 2015; Baumann *et al.*, 2017) uncovered numerous sedimentary deposits containing a high density of archaeological remains along L'Amélie beach (Verdin *et al.*, 2019). Due to the long coastal human occupation, the beaches of the North-Médoc are occasionally the subject of archaeological discoveries (Marambat, 1992; Diot *et al.*, 2001; Clavé, 2001) that testify to a complex palaeogeographic evolution of this coastal area, characterized by high shoreline mobility at the mouth of the Gironde during the Holocene period (Allen *et al.*, 1974; Pontee *et al.*, 1998). From March 2014, several campaigns of post-storm geomorphological and archaeological prospection were simultaneously undertaken on the intertidal zone of L'Amélie beach in the framework of an interdisciplinary research programme (LITAQ programme). Thus the specific objectives of the present study are (1) to detail the stratigraphy and evolution of the North-Médoc dune barrier in the light of recent archaeological finds, (2) to date both archaeological and sedimentary material, (3) to identify the major morphological changes that occurred on the south side of the Gironde estuary inlet in relation to both sea-level rise (SLR) and climatic variability, and (4) to define the effects of dune formation on coastline changes and human settlement of the North-Médoc peninsula over the last seven millennia.

2 - STUDY AREA

2.1 - THE GIRONDE ESTUARY MOUTH

The open sandy beach of L'Amélie lies south of the Gironde estuary inlet (fig. 1), which has shifted significantly landward - by an estimated 1 to 2 km / 1000 years (LCHF, 1979, 1982, 1987) over the last 3000 years - under bedrock control of the shoreline retreat. Unlike the Leyre estuary, located a hundred kilometres south of the Gironde mouth, which has shifted laterally to the south (Fénies & Lericolais, 2005), the Gironde tidal inlet has remained largely in a fixed location along a NW-SE-trending structural axis (Fénies *et al.*, 2010). The presence of resistant bedrock headlands near the inlet of the Gironde estuary (composed of Eocene carbonates, see fig. 1c) has prevented its lateral migration to the south under the influence of the prevailing southward littoral drift. As a consequence, the northern coastal barrier has shifted cross-shore over a distance of a few kilometres whereas the southern coastal barrier has migrated alongshore from the N-S-trending linear Aquitaine coastline to a SW-NE-oriented spit - the Pointe

de Grave - which divides the Gironde mouth into an inner estuary and an outer estuary. Thus the peculiar northwest orientation of this part of the Aquitaine coast must be linked to its specific location and recent morphological evolution within the inlet of the Gironde estuary.

During the mid to late Holocene, the North-Médoc peninsula exhibited morpho-sedimentary evidence of significant coastal changes near the mouth of the Gironde due to tidal channel migration and dune ridge breaching (Pontee *et al.*, 1998). Based on the exploitation of 360 geological cores, Pontee *et al.* (1998) proposed a set of three palaeogeographic maps to illustrate these coastal changes (fig. 3). The general principles of these changes were primarily established by the characterization of two generations of tidal marshes (Allard *et al.*, 1974) separated by a shelly ridge (the 'Cordon de Richard') that began

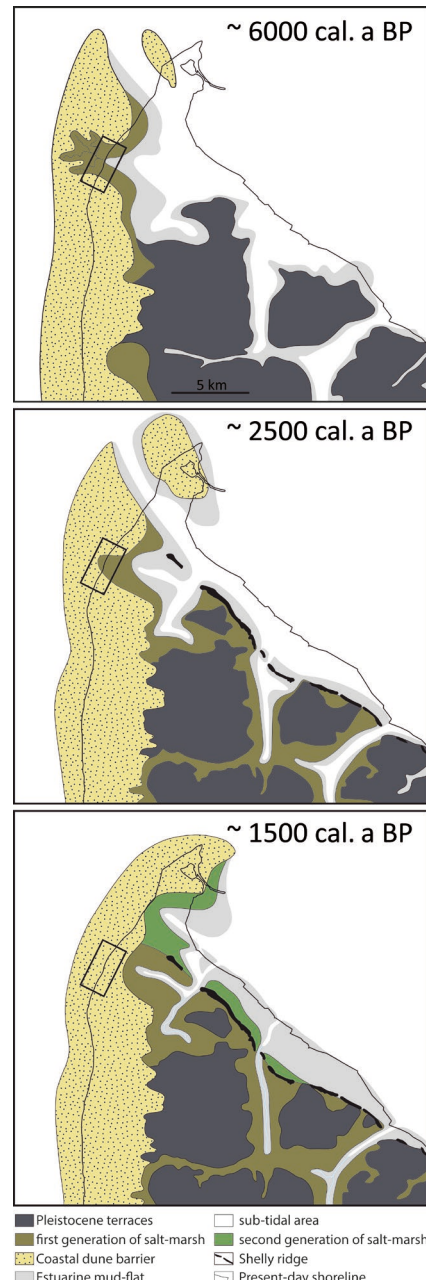
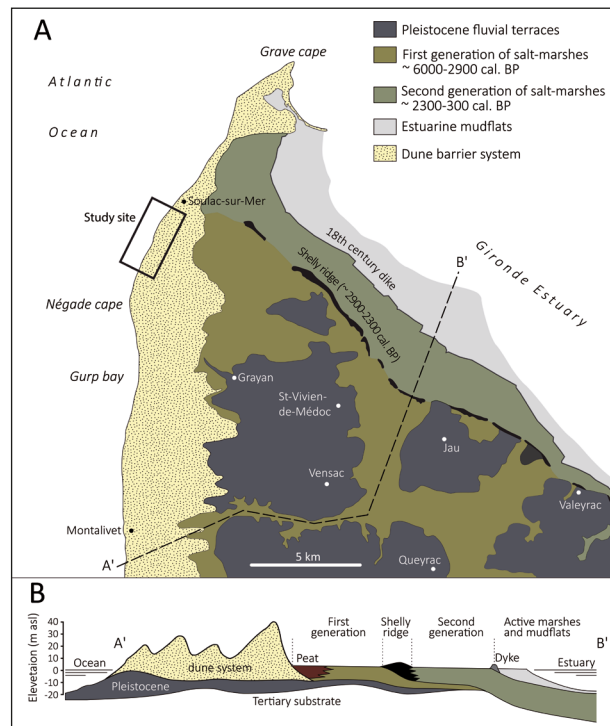


Fig. 3: Palaeogeographic reconstructions of the North Médoc peninsula from ca. 6000 to 1500 cal. a BP (from Pontee *et al.*, 1998).

*Fig. 3 : Reconstitution des changements paléogéographiques de la péninsule du Nord-Médoc de 6000 à 1500 cal BP (d'après Pontee *et al.*, 1998).*

to form ca. 2500 cal. a BP (Diot & Tastet, 1995; Massé *et al.*, 2001) (fig. 4). Sedimentation within the estuary reduced the considerable available accommodation space produced by earlier post-glacial relative sea-level (RSL) rise largely accounting for the extent of the present-day Médoc peninsula deposits (Pontee *et al.*, 1998).



Coastal changes in the area were also influenced by dune field formation and migration landwards across the Atlantic coastal zone, depositing massive amounts of sand within the transgressive systems that have predominantly filled the Gironde incised-valley. The stratigraphy and a relative chronology of the dune barrier complex of the coastal zone of North-Médoc were first based upon the morphology of the dunes (Marionnaud & Dubreuilh, 1972) and later refined based on fieldwork, new chronological data and a reanalysis of historical maps (Tastet, 1998; Clarke *et al.* 1999, 2002). The North-Médoc coastal dunes consist of two major transgressive dune fields (fig. 5). The primary dunes, invariably compound climbing parabolic dunes, were mobile during two periods (between 5000-3500 cal. a BP and between 3000-2300 cal. a BP) and then fixed by the natural development of pine forest covering the whole coastal zone until its invasion by the modern dune system. The modern dunes consist of a variety of types of crescentic dunes. Three main periods of sand drift

Fig. 4: Late Quaternary coastal formations of the North Médoc peninsula.

(A) Simplified geological map. (B) Schematic geological west–east cross-section (from Pontee *et al.*, 1998).

*Fig. 4 : Formations côtières fini-quaternaires du Nord Médoc. (A) Carte géologique simplifiée. (B) Coupe schématique est-ouest des dépôts (d'après Pontee *et al.*, 1998).*

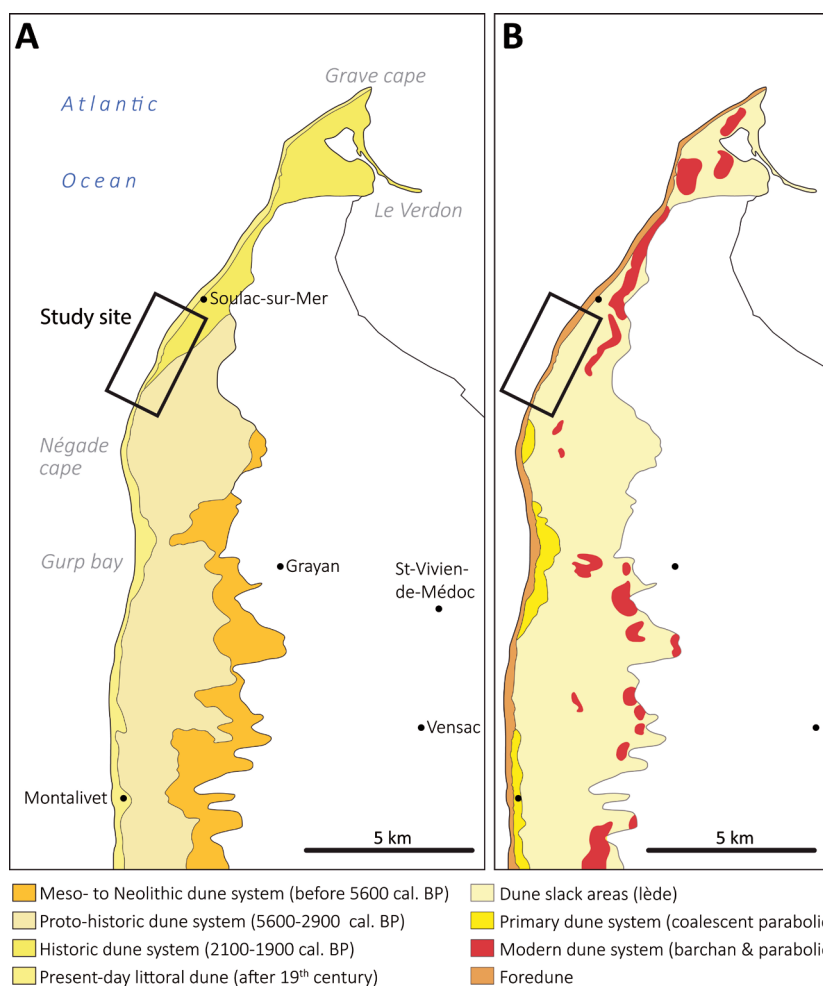


Fig. 5: Classifications of the north-Médoc coastal dune system.

(A) Classification from Marionnaud (1972) and Dubreuilh & Marionnaud (1973). (B) Revised classification from Tastet (1998) and Tastet & Pontee (1998).

Fig. 5 : Classification du système dunaire du Nord-Médoc. (A) Classification de Marionnaud (1972) et Dubreuilh & Marionnaud (1973). (B) Classification revue par Tastet (1998) et Tastet & Pontee (1998).

were recognized by authors (Tastet, 1998; Clarke *et al.* 1999, 2002): (i) around 3000-4000 cal. a BP, (ii) around 900-1300 cal. a BP and (iii) around 250-550 cal. a BP during the ‘Little Ice Age’. From the beginning of the nineteenth century, the dune ridges were stabilized by the planting of maritime pines (Buffault, 1942). In the absence of any detailed chronology of dune development and of an accurate RSL history for the region, the evolution of the Médoc peninsula has been interpreted as having formed under the influence of a series of positive and negative sea-level trends, possibly coupled with storm activity and vegetation growth (Pontee *et al.*, 1998; Clavé, 2001).

2.2 - L'AMÉLIE BEACH

The north-Médoc coast is macro-tidal with a maximal tidal range recorded at the Pointe de Grave of 5.4 m (SHOM, 2013). The wave climate is energetic, strongly seasonally modulated, with a dominant W to NW incidence (Butel *et al.*, 2002; Bertin *et al.*, 2008). High-energy winter swells and storm waves are typically from the W-NW with significant wave height sometimes exceeding 8 m, while the smaller and shorter summer waves generally arrive from the NW (Castelle *et al.*, 2014; 2015). Tidal currents are small compared with wave-induced currents, except in the close vicinity of the Soulac area where bottom tidal currents exceed 0.5 m.s⁻¹ in the Gironde inlet, but they decline rapidly on the inner shelf with values ranging from 0.10 to 0.15 m.s⁻¹ (Lesueur & Tastet, 1994).

The prevailing winds on the Médoc peninsula are WNW to WSW, representing 50 % of the total winds (Michel & Howa, 1999; Favennec *et al.*, 2002). The strongest winds reaching 26 m.s⁻¹ are recorded in winter and have an average direction between SW and NW. From sand trapping measurements, Favennec *et al.* (2002) showed around 70 % of aeolian sand volumes are transported in autumn and early spring along the Aquitaine coast. Moreover, sands of grain sizes up to 300 µm can be blown to the inner part of the dune ridge during the strongest wind events.

L’Amélie beach is a sandy beach some 2 km long and about 100 m wide, south of the Soulac-sur-Mer urban area. Like most of the beaches along the Gironde coast, L’Amélie beach is characterized by the presence of rip-dominated intertidal sandbars (e.g. Bruneau *et al.*, 2011). The sandbars are predominantly rip-channelled with rip spacing of about 300 m. The rip-channels are favourable points for observing the underlying sediment outcrops along the beach.

The dune front exhibits more than 10 m high erosion scarps indicative of the present-day shoreline retreat. Since the early eighteenth century, the shoreline of the North-Médoc peninsula has been retreating, but with high alongshore variability. For the period between 1707 and 1966, Froidefond (1982) calculated shoreline migration for different locations along the coast: Pointe de Grave (-1500 ± 370 m), Soulac-sur-Mer (-300 ± 75 m), L’Amélie beach (+100 ± 25 m), Anse du Gurp (-500 ± 125 m), Montalivet (-50 ± 25 m). For the

last decades, the shoreline sections north and south of La Négade cape (fig. 1) have displayed different migration patterns (Aubié & Tastet, 2000). The southern section is dominated by southward longshore drift and the maximum erosion rate is about 7 m/yr in its northern part, decreasing southward to about 1-2 m/yr at Lacanau (fig. 1). The section north of La Négade cape on the other hand is dominated by northward longshore drift and recorded shoreline retreat rates were about 5-10 m/yr from the 1960s to the 1990s (Aubié & Tastet, 2000). More recently, Castelle *et al.* (2018) have calculated multidecadal shoreline changes along the Aquitaine coast from a set of orthorectified aerial photographs and highlighted a higher sensitivity to erosion for beaches located close to the estuarine mouths. German bunkers located about 100 m seaward from the present-day shoreline are indicative of this historical coastal erosion. The eroded coastal sediments are transported by longshore drift to subtidal areas of the Gironde mouth where the sand supply is estimated to be 1.8 10⁶ m³/yr (Allen *et al.*, 1981). Idier *et al.* (2013) highlighted the strong interannual variability of the shoreline dynamics of the Aquitaine coast. Storm periods appear to be responsible for an acceleration of the retreat rates. The example of the severe storms of winter 2013-2014 is illustrative, with mean values of retreat around 20 m along the coast of Soulac-sur-Mer and maximum retreat values reaching 40 m on L’Amélie beach (Bulteau *et al.*, 2014). In response to the recent coastal erosion, several defence structures have been installed along the coast in front of urbanized areas.

2.3 - COASTAL ARCHAEOLOGICAL REMAINS OF HUMAN SETTLEMENTS

Along the northern coast of the Médoc, erosion of Holocene estuarine silty-sediment intertidal deposits has uncovered plentiful evidence of past human settlements dating from the Mesolithic (10600-8000 cal. a BP) to the end of Antiquity (1450-1350 cal. a BP) (Marambat, 1992; Clavé, 2001). The high density of archaeological remains in coastal areas is attested by the numerous field discoveries reported by non-professional archaeologists. The lack of any real archaeological research programme has led to some confusion about the data acquired in this area. These findings were re-examined on the basis of the knowledge gained from the LITAQ programme in order to better understand the dynamics of settlement and the nature of the activities practised in the estuarine marshes (Verdin *et al.*, 2019). In the Mesolithic and early Neolithic periods (8000-6500 cal. a BP), human settlements were located essentially around the sites of La Négade cape (Lède du Gurp) and Le Gurp Bay (fig. 1b). From the middle Neolithic and the late Neolithic (6500-4200 cal. a BP), the coastal area located between the localities of Soulac-sur-Mer and Montalivet displays a high density of archaeological sites, associated with a large scale practice of salt mining. The middle Bronze Age (3600-3400 cal. a BP) saw intense frequentation of the estuarine marshes for a purpose that is not yet well defined. Salt production is likely, but it is not truly evidenced by

archaeological data. Numerous deposits of axes testify to a flourishing metallurgical industry and the coast of North Médoc perhaps lay at the crossroads of maritime and terrestrial communication routes for the trading of metals. The final Bronze period (3400-2800 cal. a BP) corresponds to a break in the human occupation of the Médoc coastal zone. In the Iron Age (2500-1950 cal. a BP), the archaeological evidence of past activities resumed with numerous signs of production of ignigenous salt. Finally, in Antiquity (1950-1450 cal. a BP), the human settlements are associated with shellfish deposits, especially oysters, the harvesting of which could explain, among other things, the regular frequentation of these locations.

3 - MATERIALS AND METHODS

3.1 - TOPOGRAPHY

3.1.1 - DGPS Surveys

During the field campaigns, Differential Global Positioning System (DGPS) surveys were systematically conducted to obtain homogenously spread information about geomorphological and archaeological discoveries (contours of sediment outcrops on the beach, archaeological remains, dune palaeosols, sediment samples, position of beach cores, excavation by mechanical digger, etc.). Surveys were carried out using (i) a Trimble 5700/5800 Differential GPS in March and June 2014, and (ii) a Topcon Hyper V Differential GPS in March 2015. Data points described by three coordinate values (x, y, z) were collected in Real Time Kinematic (RTK) mode with an accuracy of, respectively, 4-5 cm (x and y) and 1 cm (z) (Suanez *et al.*, 2012).

Each DGPS measurement was converted into the French Lambert 93 coordinate system and elevations were linked to the French national datum NGF (*Nivellement Général Français*). Data were converted with respect to a benchmark installed on the jetty of L'Amélie beach during the first field campaigns in March 2014. The absolute geographical coordinates of the benchmark were obtained from a post-processing procedure using GrafNet 8.3 software. The raw GPS base data were stored and processed against raw GPS files provided

by the permanent GPS network GNSS (IGN) for fixed stations close to the study site. The accuracy of the post-processing procedure is estimated to be within 1 cm.

3.1.2 - Terrestrial Laser Scanning (TLS) methodology

Five campaigns of TLS data acquisition were undertaken between March 2014 and March 2015 to cover the studied coastal area (tab. 1). Ground-based laser scanner systems use LiDAR (light detection and ranging) technology to provide very accurate measurements of an object's range relative to the scanner position (Watt & Donoghue, 2005). This is achieved by recording the time taken for the laser pulse to hit the target and return to the sensor (laser head) (Lichti *et al.*, 2002). Provided that the location and orientation of the sensor head are known at the time of the survey, the scan data can be spatially registered to any given coordinate system. For these reasons, TLS is a useful tool for the acquisition of accurate topographic measurements on morphological features that are difficult to survey such as dune cliffs (fig. 6).

In this study, scans were recorded using a Riegl VZ400 high-speed laser scanning system linked to a laptop computer. This scanner has a vertical and horizontal scanning range of 100° (Theta angle) and 360° (Phi angle) respectively. The scanning rate can be varied depending on the spatial resolution required, with a maximum data capture rate of up to 120000 points per second. The near-horizontal surfaces of the beaches were scanned with a medium resolution ranging from 0.04° to 0.10° for Theta and Phi angles respectively. Higher resolutions, between 0.02° and 0.06°, were used to scan the vertical face of the dune cliffs and obtain a better picture of the dune section. Data obtained in the form of a point cloud constitute a 'model space' with an accuracy of distance from the point location of up to 4 mm and spatial 3D up to 6 mm. A digital camera with a capacity of 5 MP was incorporated in the TLS allowing us to take a spherical photograph of the scanned area during one measurement cycle. The compatibility of distance measurement with the panoramic image enables multi-aspect analysis of the Digital Surface Model and spherical photograph of the surrounding area using RISCANPRO 1.8 software.

Dates	Material	Data obtained	Number of TLS scan position	Number of data points (10 ⁶)	Location	overall scan		fine scan (dune)	
						Vertical angle	Horizontal angle	Vertical angle	Horizontal angle
3/19/2014	TLS (Riegl VZ400)	beach/dune topography	2	6.5	centre of L'Amelie beach	0.06	0.06	0.02	0.02
3/20/2014	TLS (Riegl VZ400)	beach/dune topography	2	12.1	south of L'Amelie beach	0.06	0.06	0.04	0.04
6/17/2014	TLS (Riegl VZ400)	beach/dune topography	5	6.4	north of L'Amelie Beach	0.1	0.1	0.05	0.05
3/20/2015	TLS (Riegl VZ400)	beach/dune topography	3	12.5	south of La Glaneuse beach	0.04	0.06	0.04	0.04
3/21/2015	TLS (Riegl VZ400)	beach/dune topography	6	23.1	centre of La Glaneuse beach	0.04	0.06	0.04	0.04

Tab. 1: Details of TLS surveys made along L'Amélie beach.

Tab. 1 : Détails des relevés TLS effectués le long de la plage de l'Amélie.

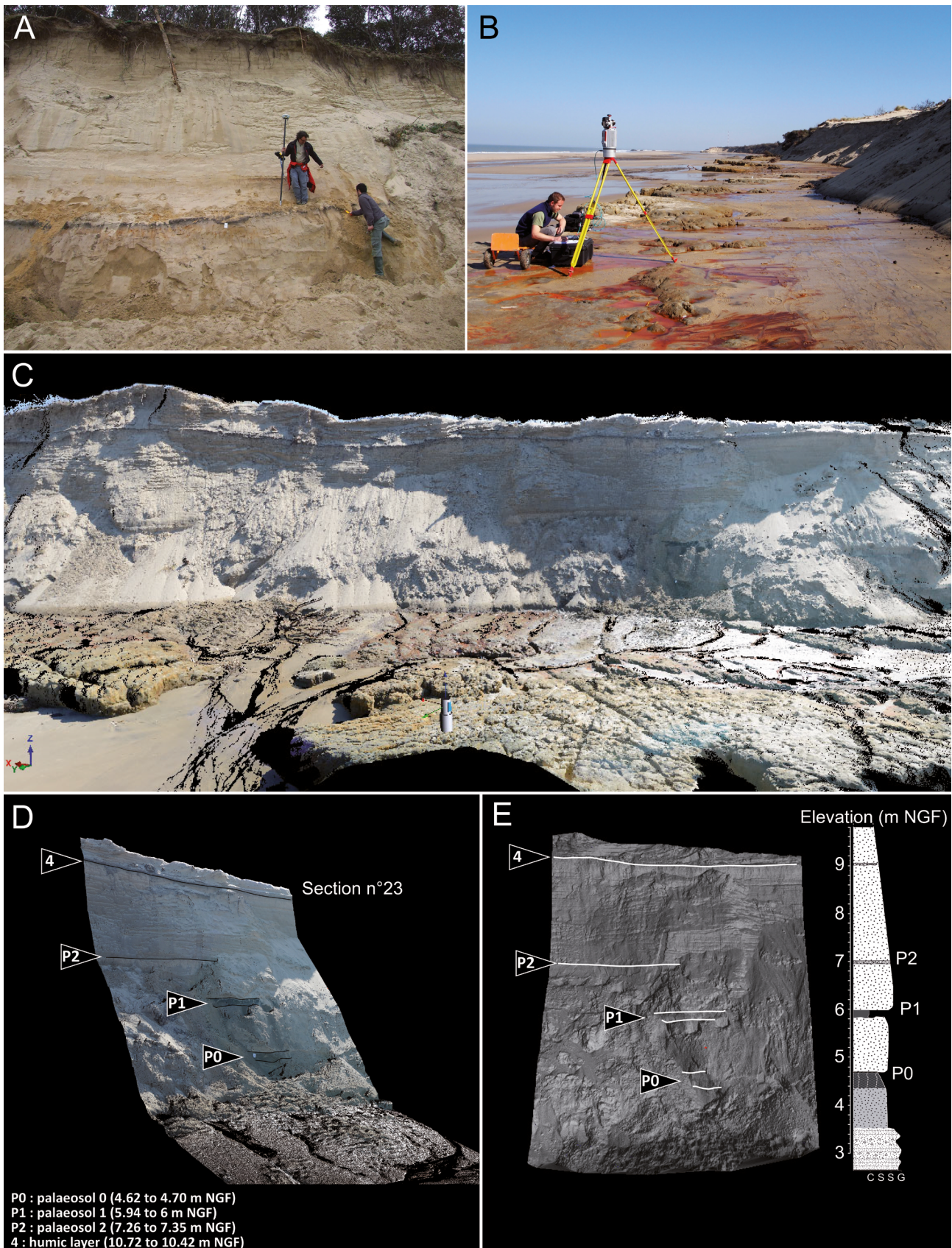


Fig. 6: Topographic surveys along the L'Amélie dune front.

(A) DGPS measurements. (B) TLS measurements. (C, D, E) High density point clouds obtained from TLS survey (here in section 23). The elevations of each aeolian sand unit and interbedded palaeosols and/or humic layers were easily obtained. All studied sections were correlated to propose a continuous 2 km alongshore stratigraphic view.

Fig. 6 : Relevés topographiques le long du front de dune de l'Amélie. (A) Mesures au DGPS. (B) Mesures au TLS. (C),(D) et (E) : Nuage de points de forte densité obtenu à partir d'un relevé au TLS (ici au niveau de la section 23). Les altitudes de chaque unité de sable éolien et de paléosol et/ou horizon humique interstratifiés ont été facilement obtenues. Toutes les sections étudiées ont été corrélées afin de proposer une vue stratigraphique continue sur 2 km de linéaire côtier.

Using TLS for measuring large areas involves integrating data obtained from individual measurement sites (Kociuba *et al.*, 2014). In this study, the TLS data were acquired from 18 different locations spaced 100 m apart at most to ensure an adequate overlap of the separate point clouds along the entire length of the two beaches surveyed. The total area covered by our TLS surveys is around 50 ha and the topographic measurements extend over a distance of about 2270 m along the coast. A target point (TP) method was applied to merge the consecutive point clouds. This method is based on the distribution of a set of reflective targets in the field before TLS acquisition. The reflective targets we used were plastic tubes measuring 10 cm in diameter. The target network was recognized by the scanner after selection of a relevant function of the scanning software. In parallel, the geographical position of each target was measured by means of a differential GPS (Trimble 5700-5800 in 2014, Topcon Hyper V in 2015) allowing georeferencing of individual point clouds. Thus, all the point clouds were replaced in the same geographical coordinate system corresponding to Lambert 93 and elevations were connected to the French altitudinal datum (NGF). The maximum errors of the model came to 0.043 m horizontally and 0.053 m vertically.

Finally, to facilitate the integration of data in a GIS, measured data in the form of a point cloud were transformed into a Digital Elevation Model (DEM) of the entire scanned area. The DEM was constructed with a resolution of 0.4×0.4 m using a gridding interpolation method.

3.2 - SEDIMENT ANALYSIS

Grain-size analyses were performed in two different laboratories. However, the protocol analysis was identical in both cases. The grain-size distribution of 72 sediment samples collected along the dune cliff was measured at the Laboratoire de Géographie Physique de Meudon (LGP, UMR 8591 CNRS) using a Beckmann-Coulter LS230 laser granulometer for the fine fraction (<1 mm) and a sieving procedure for coarse material (>1 mm). A total of 30 sediment samples from the beach outcrops were analysed in the LETG (UMR 6554 CNRS) laboratory using a Malvern Mastersizer 2000 laser analyser. Organic matter was removed for laser-diffraction particle size study with hydrogen peroxide pre-treatment (e.g. Scott-Jackson & Walkington, 2005; Wang *et al.*, 2006). All of the samples were mixed with a dispersing agent (0.3 % sodium hexametaphosphate) in order to disperse the clay particles.

The formulas proposed by Folk and Ward (1957) were used to calculate the main grain-size characteristics: median (D50), sorting (σ_g), skewness (SKI) and kurtosis (KG) index values. For micropalaeontological analysis, 17 sediment samples were sieved through a 500 μm and 63 μm mesh and washed to remove clay and silt material. Foraminifera were concentrated by flotation in trichloroethylene as described by Murray (1979).

Where possible, a minimum amount of 300 specimens of foraminifera were counted under a stereoscopic binocular microscope. Species identification was mainly based on specific papers showing modern assemblages and their distribution patterns in NE Atlantic estuaries and salt marshes (Allen *et al.*, 1974; Moulinier, 1996; Redois & Debenay, 1996; Goubert, 1997; Armynot du Châtelet *et al.*, 2005; Duchemin *et al.*, 2005; Debenay *et al.*, 2006; Leorri *et al.*, 2010; Rossi *et al.*, 2011; Delaine *et al.*, 2015). Ostracod species were identified by the same approach (Oertli, 1985; Ruiz *et al.*, 2000; Allen *et al.*, 1974; Carbonel, 1980; Clavé *et al.*, 2001).

3.3 - RADIOCARBON DATING

A total of 14 carbon-rich sediment samples were collected from the field and radiocarbon dated at the VERA Laboratory (University of Vienna, Austria) and at the Beta-Analytic laboratory (Miami, USA) (tabs. 2 & 3). The conventional radiocarbon dates were calibrated using software Calib 7.0 (Stuiver & Reimer, 1993) and the IntCal13 calibration curve (Reimer *et al.*, 2013). Errors in the inferred radiocarbon dates cannot be excluded, especially on the bulk palaeosol samples, because of the possible contamination of the sediment by older or younger carbon, such as by rootlet penetration or inwashed material. Two marine shells were also radiocarbon dated, taking into account the local reservoir effect. The Marine13 calibration curve was used and a delta R value of -10 (Standard Deviation = 37) was estimated from the Marine Reservoir Correction Database (Reimer *et al.*, 2013) by using the nine nearest measurement points located less than 200 km from our study site (Tisnérat-Laborde *et al.*, 2010). Finally, the radiocarbon results and the chronologically well-defined archaeological remains were used to provide a reliable chronological framework of the Holocene sediment infilling of L'Amélie beach.

3.4 - SEA-LEVEL INDEX POINTS PRODUCTION

Sedimentological analysis, radiocarbon dating and accurate elevation measurements of coastal deposits and the associated archaeological remains were used to propose some new Holocene RSL data from this part of the French Atlantic coast. Holocene relative sea-levels were reconstructed using the ‘sea-level index point’ (SLIP) methodology (Hijma *et al.*, 2015). The RSL for a SLIP is calculated from:

$$\text{RSL} = \text{Es} - \text{RWLs}$$

where Es and RWLs are the elevation and reference water level of samples, expressed relative to the same datum, and RSL is relative to local sea level at the time of sampling. The reference water level is the mid-point of the indicative range (IR) considered as the elevational range over which an indicator forms. Table 4 presents all the data used to produce our RSL records. The database is structured in the same format as that proposed for the Atlantic coasts of Europe (García-Artola *et al.*, 2018).

N°	Lab. code	Location		Elevation Z (m NGF)	Archaeo- logical location	Strati- graphic unit	material dated	Age (BP)	+/-	cal. a BP			Cultural period	Reference
		X	Y							min.	med.	max.		
1	Beta-463940	376869.01	6497581.34	-1.16;-2.16	AML-N-003	US2b	rootlets (bulk)	6360	30	7183	7292	7416	Early Neolithic	This study
2	VERA-51400	376861.44	6497720.83	-0.23	AML-N-003	US3b (base)	wood	6025	50	6742	6869	6996	Early Neolithic	This study
3	VERA-51404	376243.41	6496392.46	3.35	AML-N-001	not defined	charcoal	5040	130	5482	5790	6176	Mid to late Neolithic	This study
4	VERA-51336	376928.04	6497843.10	-0.53	AML-N-004	US3b (top)	wood (Quercus)	3984	70	4236	4455	4802	Late Neolithic	This study
5	*	*	*	*	AML-N-008	US3d	Scrobicularia shell	3390	60	3070	3263	3434	Late Bronze Age	Clavé (2001)
6	VERA-51402	376558.08	6497282.48	-1.45	AML-N-008	US3b	wood	2570	40	2495	2716	2762	Early Iron Age	This study
7	VERA-51338	376611.48	6497185.43	-0.08	AML-N-007	US4	oyster shell	2108	74	1510	1701	1897	Gallo-Roman / Antiquity	This study
8	VERA-51397	376895.24	6497719.08	1.34	AML-N-003	U5	wood	1260	50	1070	1203	1286	Early Middle Ages	This study

Tab. 2: Details of radiocarbon ages obtained from samples collected on the sediment outcrops along L'Amélie beach.

Geographic coordinates of sampled points are in the French Lambert 93 coordinate system and elevations were attached to the French national datum NGF (*Nivellement Général Français*) corresponding to the mean sea level. Shaded rows correspond to marine shell samples whose radiocarbon ages were calibrated using the MARINE13 calibration curve with a ΔR of -10 and a standard deviation of 37 (see text for details).

Tab. 2 : Détails des datations radiocarbone obtenues à partir des échantillons prélevés sur les affleurements sédimentaires le long de la plage de l'Amélie. Les coordonnées géographiques des points de prélèvement sont données dans le système Lambert 93 et les altitudes sont raccordées au niveau de référence NGF. Les lignes grisées correspondent aux échantillons de coquilles marines dont les âges radiocarbones ont été calibrés à partir de la courbe de calibration MARINE13 en utilisant une valeur ΔR de -10 et une déviation standard de 37 (voir le texte pour plus de détail).

Lab. Code	Location		Elevation Z (m NGF)	Terrain code	Stratigraphic unit	Material dated	Age (BP)	+/-	cal. a BP			Cultural period
	X	Y							min.	med.	max.	
VERA-51333	376485.97	6496713.67	5.70	section 16	Dune palaesol 1	palaesol (bulk)	1178	70	963	1106	1263	early middle ages
VERA-51335	376667.86	6497052.65	4.45	section 4	Dune palaesol 1	palaesol (wood)	1089	69	802	1012	1180	early middle ages
VERA-51334	376682.13	6497087.05	4.52	section 3	Dune palaesol 1	palaesol (bulk)	1328	51	1097	1257	1344	early middle ages
VERA-51339	376352.48	6496535.78	4.85	section 21	Dune palaesol 0	palaesol (bulk)	1921	71	1638	1866	2041	Late Iron Age to Early Empire
VERA-51337	376194.64	6496314.88	4.52	section 25	Dune palaesol 0	palaesol (bulk)	2026	65	1828	1988	2148	Late Iron Age to Early Empire
VERA-51398	376101.83	6496141.32	3.75	section 28	Dune palaesol 0	peat	1735	45	1542	1648	1780	Antiquity-Gallo-Roman
VERA-51401	376623.69	6496963.51	-2.90	Pied de dune 1	Dune palaesol 0	peat	1720	120	1371	1639	1893	Antiquity-Gallo-Roman

Tab. 3: Details of radiocarbon ages obtained from samples collected on the dune palaeosols of L'Amélie beach.

Geographic coordinates of sampled points are in the French coordinate system Lambert 93 and elevations are related to the French national datum NGF (*Nivellement Général Français*) corresponding to the mean sea level.

Tab. 3 : Détails des datations radiocarbone obtenues à partir des échantillons prélevés sur les paléosols dunaires de la plage de l'Amélie. Les coordonnées géographiques des points de prélèvement sont données dans le système Lambert 93 et les altitudes sont raccordées au niveau de référence NGF.

In this study, the IR was defined for three sediment samples using the palaeoenvironmental information provided by the foraminiferal assemblages. The IR is ranged from (i) mean high water neap tide (MHWNT) to highest astronomical tide (HAT) for assemblages indicative of a high salt marsh depositional environment, (ii) from mean low water spring tide (MLWST) to mean high water spring tide (MHWST) for assemblages dominated by tidal flat species; and (iii) above HAT for archaeological remains associated with human occupation or funeral practices, considered as a limiting point.

The tide levels were defined by the French Hydrographic and Oceanographic Institute (SHOM, 2016) for the locality of Royan, located 15 km north of the study area. The uncertainty for the vertical position

of RSL was quantified by taking into account: (i) the IR, (ii) the sample thickness, (iii) the sampling uncertainty, (iv) the uncertainty associated with the calculation of the elevation from DGPS and TLS measurements. We did not apply any corrections for tidal range variation in the past.

4 - RESULTS

4.1 - CARTOGRAPHY AND STRATIGRAPHY OF INTERTIDAL SEDIMENT DEPOSITS

Based on field observations, DGPS surveys and sedimentological analyses (grain-size analysis, sedimentary

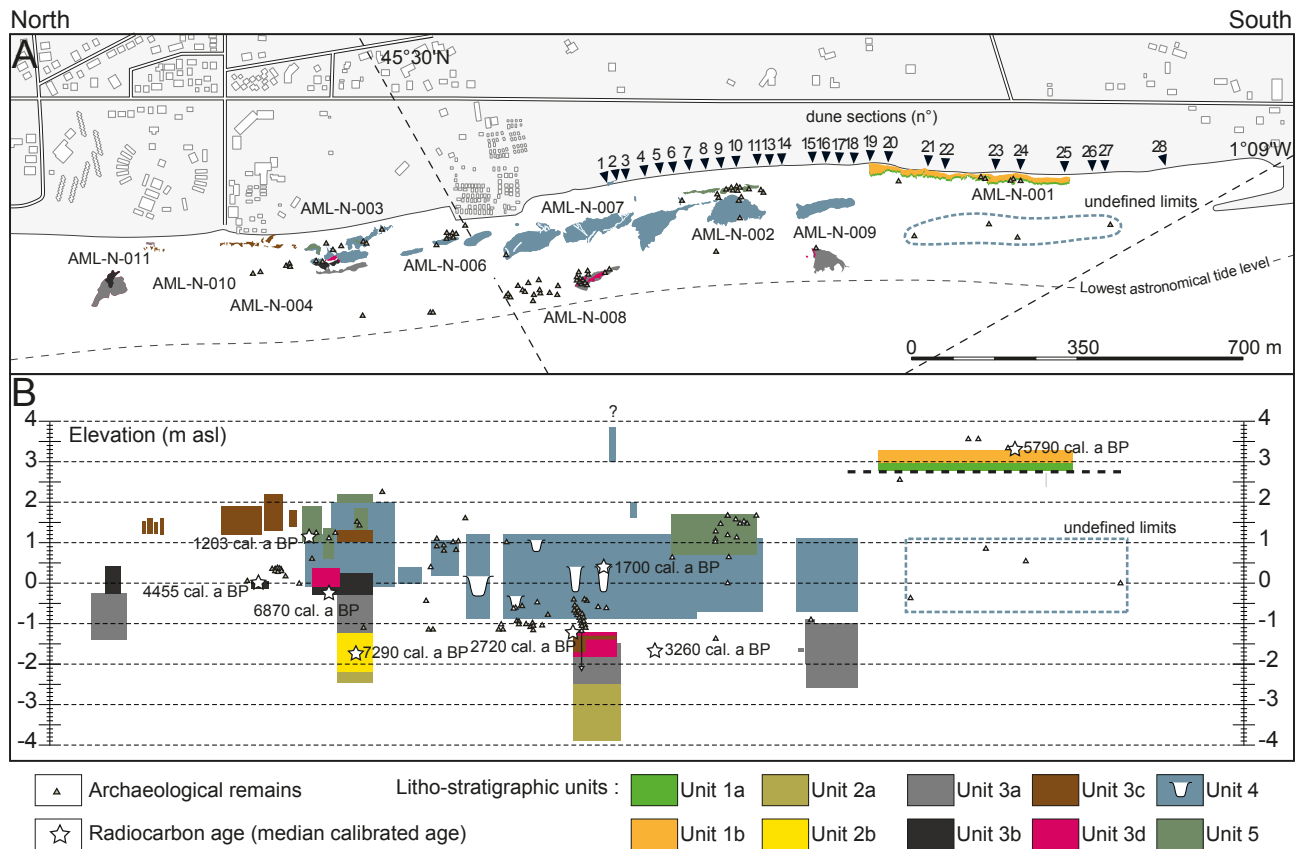


Fig. 7: Archaeological sites and sedimentary outcrops measured along L'Amélie beach.

(A) Location map. (B) Vertical projection of the alongshore and elevational limits of the sedimentary units offering a stratigraphic view of deposits. The dune sections studied are also located along the dune front.

Fig. 7 : Sites archéologiques et unités sédimentaires à l'affleurement le long de la plage de L'Amélie. (A) Carte de localisation. (B) Projection verticale des limites spatiales et altitudinales des unités offrant une vision stratigraphique des dépôts. Les sections dunaires étudiées sont également localisées le long du front de dune.

structures, organic and micropalaeontological content, radiocarbon dating) the sediment deposits cropping out along the beaches of L'Amélie and La Glaneuse were subdivided into 10 main lithofacies (U1 to U10, fig. 7). The cartography and the accurate elevation measurements were used to propose a general framework of the stratigraphic succession of deposits for the study area. The interpretation in terms of depositional environments was based on classic models (Reineck & Singh 1980; Allen 2000, 2003), regional studies of estuarine and coastal areas (e.g. Lespez *et al.* 2010; Tessier *et al.* 2012; Stéphan *et al.*, 2015) and comparison with modern sediments characterizing coastal environments along the Gironde estuary (e.g. Marionnaud & Dubreuilh, 1972; Diot & Tastet, 1995; Massé *et al.*, 2001). Archaeological remains discovered during field campaigns helped to better interpret the chronostratigraphic context of the sediment successions.

4.1.1 - Unit 1: Pleistocene deposits

The oldest sedimentary successions (unit 1) corresponds to Pleistocene deposits represented by a 2 m thick compact dark-green clay (unit 1a) overlain by a 60 cm to 1 m thick gravelly sandstone (unit 1b) (fig. 8a). Unit 1a was only observed in the south of L'Amélie beach and was attributed to an estuarine mudflat sediment dated to MIS9 from the combination

of luminescence (OSL, IR-RF) and electron spin resonance (ESR) dating of quartz and feldspar grains (Bosq *et al.*, 2019). The median grain size is 8 µm. These sedimentological characteristics are consistent with results obtained by Marionnaud and Dubreuilh (1972). Unit 1b is a gravelly sandstone, 1.1 m thick at most observed only in the south of L'Amélie beach at the base of the dune front. This deposit is a colluvial material (Grès de l'Amélie) dated to the Weichselian Pleniglacial (MIS 2, Bosq *et al.*, 2019). Numerous archaeological remains were discovered on the top of this deposit (ceramic fragments and flints attributed to the Bronze Age). A pit, dug in the sandstone and containing many wooden poles, was excavated on site AML-N-001 (fig. 9a) and a coal gave a radiocarbon age of 6180-5480 cal. a BP (mid to late Neolithic).

4.1.2 - Unit 2: Early Neolithic tidal inlet (7410-7180 cal. a BP)

Unit 2 corresponds to the first stage of the Holocene estuarine sediment infilling of L'Amélie and La Glaneuse beaches. The basal sediment unit (unit 2a) is a very well sorted (σ_g between 0.62 and 1.08) medium to coarse sand with a mean grain size ranging from 490 µm to 1010 µm (fig. 10). In detail, the mean grain size decreases from the bottom to the top of the deposit, which is characteristic of the filling of a tidal channel. Unit 2 was encountered

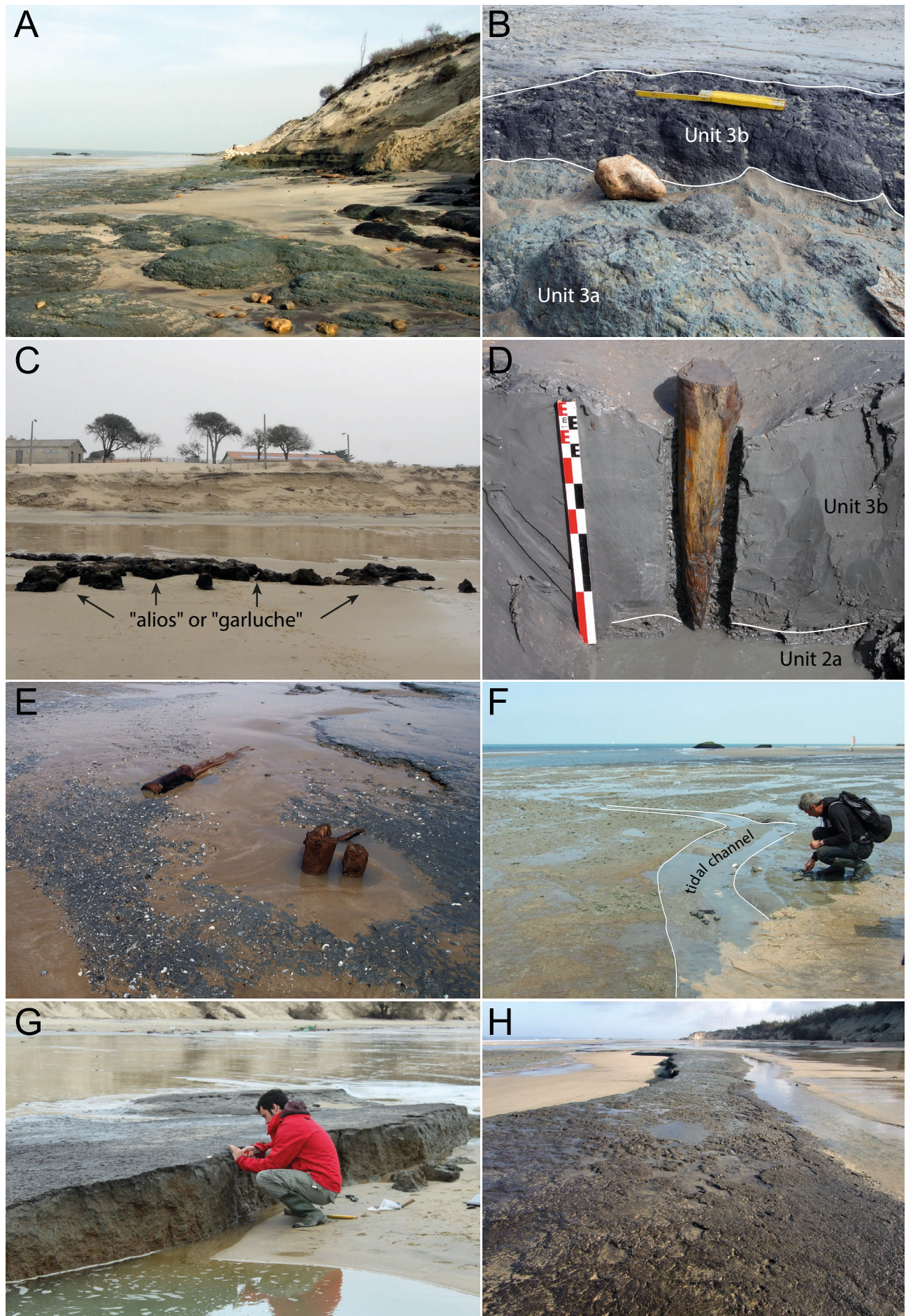


Fig. 8: Photographs illustrating the sediment deposits outcropping along L'Amélie beach.

(A) Green clay (unit 1) uncovered during the winter 2014 in the south of L'Amélie beach (21/03/2015, P. Stéphan). This unit is attributed to the “Argiles du Gurl” Pleistocene formation (Marionnaud & Dubreuilh, 1972; Beauval *et al.*, 1998; Tastet, 1999). (B) Sharp contact between the green clay (unit 3a) and the organic-rich silty-clay (unit 3b) in the north of L'Amélie beach (archaeological site AML-N-003, 22/03/14, O. Got). (C) Cemented aeolian sand (“aliots” or “garluche”) cropping out in the north of L'Amélie beach (21/03/2015, P. Stéphan). (D) Oak post mechanically excavated at the lowest tide level of L'Amélie beach. The post is fixed into a blue silty clay (unit 3b) overlying a coarse sand deposit (unit 3a) (archaeological site AML-N-008, 23/03/2015, P. Stéphan). (E) Silty clay with high proportion of fragmented Scrobicularia shells observed at the low spring tide level in the central part of L'Amélie beach (archaeological site AML-N-008, 23/03/15, P. Stéphan). (F) Silty clay deposit (unit 4) cropping out at the mean tide level in the central part of L'Amélie beach (archaeological site AML-N-007, 18/06/2014, F. Verdin). The surface of the deposits exhibit several tidal channels filled with oyster shells. (G) Organic silty-clay (unit 5) uncovered by marine erosion at the high neap tide level (archaeological site AML-N-002, 17-22/03/2014, F. Verdin). (H) Organic-rich surface of unit 5 showing numerous animal footprints (archaeological site AML-N-002, 17-22/03/2014, F. Verdin).

Fig. 8 : Photographies illustrant les dépôts sédimentaires affleurant le long de la plage de l'Amélie. (A) Argile verte (unité 1) mise au jour lors de l'hiver 2014 dans le sud de la plage de l'Amélie. Cette unité est attribuée à la formation pléistocène des « argiles du Gurl » (Marionnaud et Dubreuilh, 1972; Beauval *et al.*, 1998; Tastet, 1999). (B) Contact net entre les argiles vertes (unité 3a) et l'argile limoneuse organique (unité 3b) dans le nord de la plage de l'Amélie (site archéologique AML-N-003, 22/03/14, O. Got). (C) Sable éolien induré (« aliots » ou « garluche ») affleurant dans le nord de la plage de l'Amélie (21/03/2015, P. Stéphan). (D) Poteau en chêne mis au jour mécaniquement au niveau des plus basses mers de vive-eau sur la plage de l'Amélie. Le poteau est planté dans un limon argileux bleu (unité 3b) qui repose sur un dépôt de sable grossier (unité 3a) (site archéologique AML-N-008, 23/03/2015, P. Stéphan). (E) Limon argileux à forte proportion de coquilles de scrobiculaires fragmentées (unité 3d) observé en bas de plage dans la partie centrale du secteur de l'Amélie (site archéologique AML-N-008, 23/03/15, P. Stéphan). (F) Limon argileux (unité 4) affleurant au niveau de mi-marée au centre de la plage de l'Amélie (site archéologique AML-N-007, 18/06/2014, F. Verdin). La surface de ce dépôt montre plusieurs chenaux de marée comblés par des coquilles d'huîtres. (G) Limon argileux organique (unité 5) mis au jour par l'érosion marin au niveau des pleines mers de morte-eau (site archéologique AML-N-002, 17-22/03/2014, F. Verdin). (H) Surface très organique de l'unité 5 montrant de nombreuses empreintes d'animaux (site archéologique AML-N-002, 17-22/03/2014, F. Verdin).

at an elevation ranging from -3.9 to -2.5 m asl, during a mechanical excavation of the lowest part of L'Amelie beach (fig. 8d). No foraminifera were found within the sediment. A second mechanical excavation on La Glaneuse beach revealed a northward extension of this coarse sand deposit at an elevation ranging from -2.45 to -2.15 m asl. The material is overlain by a silty sand layer containing rootlets (unit 2b) dated to 7420-7180 cal. a BP (early Neolithic) (tab. 2). This unit is interpreted as the deepest fill of a large tidal channel, recognized in this area by Allen *et al.* (1974) and named the ‘Soulac channel’. This deposit is thought to be an extension of the tidal ravinement surface recognized in the outer estuary (Allen & Posamentier, 1993; Lercolais *et al.*, 1998; Feniès *et al.*, 2010) that was formed when the rate of the RSL rise slowed down around 7000 cal. a BP.

4.1.3 - Unit 3: first generation of intertidal estuarine deposits (late Neolithic to the early Iron Age)

Unit 3 consists of intertidal estuarine sediments that can be subdivided into four main sediment facies.

4.1.3.1 - Unit 3a

Unit 3a is located at an elevation ranging from -2.5 to -0.9 m asl, close to the lowest astronomical tide level (figs. 7 & 8d). Six sediment samples were collected from the base to the top of this unit during mechanical excavation of the archaeological site AML-N-008. The grain-size analysis indicates a gradual change from a sandy-silt at the base of the unit (median grain size from 30 to 40 µm) to a clayey-silt at the top (median grain size from 10 to 13 µm) with bi-modal grain-size distribution curves (fig. 10d). The first mode is between 10 and 20 µm and corresponds to a low-energy depositional environment. The second mode ranges from 200 to 400 µm and could be associated with aeolian sand supplies from a seaward sediment source or stronger tidal influences. The sand fraction decreases from the base to the top of the unit, probably due to the progressive fixation of the dune front or an increase in the distance to the

shoreline in a context of dune barrier progradation. The assemblages of foraminifera are dominated by estuarine intertidal mudflat species such as *Haynesina germanica* and *Trochammina inflata* (fig. 10e). Two brackish water species of ostracods are also present (*Cyprideis torosa* and *Loxoconcha elliptica*). We consider unit 3a to have formed in an intertidal mudflat environment behind a progradational dune barrier. A radiocarbon age obtained from a pit lined with wooden stakes at the top of this unit (archaeological site AML-N-008) gives an age of 2760-2490 cal. a BP and provides a *terminus ante quem* to the deposit around the first Iron Age.

4.1.3.2 - Unit 3b

Unit 3b is a dark organic-rich clayey-silt to silty sand (fig. 8b) with a median grain size ranging from 20 to 60 µm (fig. 10). The foraminiferal assemblage is dominated by high salt marsh species (*Trochammina inflata* and *Jadammina macrescens*). This deposit crops out only at La Glaneuse beach at an elevation ranging from -0.25 to +0.2 m asl. A wood fragment collected from the base of the unit is dated to 7000-6740 cal. a BP (tab. 2). A pit with oak wood walls was discovered at the top of this deposit (fig. 9c, d) and the wood was radiocarbon dated to 4800-4240 cal. a BP (Late Neolithic, site AML-N-004). Several marks of agricultural practices were observed on the surface, but it is possible that they were produced during a later phase of human occupation. Consequently, unit 3b may correspond to a late Neolithic high marsh environment, gradually replaced by an undifferentiated (high or low) salt marsh environment.

4.1.3.3 - Unit 3c

Unit 3c consists of a humate-impregnated black sandstone cropping out on the northern part of La Glaneuse beach (fig. 8c). The elevation of the sandstone outcrop ranges from +1.2 to +2.2 m asl (fig. 7). The sediment is well-sorted with a median grain size of 450 µm. These sedimentological characteristics are consistent with an aeolian origin (Vincent, 1996). This deposit



Fig. 9: Photographs illustrating the high density of archaeological remains along L'Amélie and La Glaneuse beaches.

(A) Neolithic pit being surveyed (archaeological site AML-N-001) (photo: F. Verdin, 23/03/2015). (B) General view of the pole structure observed at the lowest astronomical tide level (photo: F. Verdin, 23/03/15). (C) Gabion, pit and stakes (archaeological site AML-N-003) (photo: F. Verdin, 09/04/2012). (D) Gabion, pit and stakes being cleared (archaeological site AML-N-004) (photo: O. Got, 22/03/14). (E) Pot dating back to late antiquity discovered in unit U4 (archaeological site AML-N-006) (photo: F. Verdin, 18/06/2014). (F) Animal footprints visible at the top of unit U5 (archaeological site AML-N-002) (photo: Yoann Ceinturet, 08/04/2015).

Fig. 9 : Photographies illustrant la forte densité de vestiges archéologiques le long des plages de l'Amélie et La Glaneuse. (A) Site AML-N-001, contours de la fosse ST1 en 2015 et 2016 (cliché : F. Verdin, 23/03/2015). (B) Vue générale de la structure sur poteaux observée à la limite des plus basses mers (site archéologique AML-N-008) (cliché : F. Verdin, 23/03/15). (C) Gabion, fosse et piquets (site archéologique AML-N-003) (cliché : F. Verdin, 09/04/2012). (D) Gabion, fosse et piquets en cours de dégagement (site archéologique AML-N-004 (cliché : O. Got, 22/03/14). (E) Pot datant de l'Antiquité tardive dégagé dans l'unité U4 (site archéologique AML-N-006) (cliché : F. Verdin, 18/06/2014). (F) Empreintes animales visibles au sommet de l'unité U5 (site archéologique AML-N-002) (Photo : Yoann Ceinturet, 08/04/2015).

could be interpreted as an ‘*alias*’ or as a bog iron (called ‘garluches’ in the Aquitaine area). The ‘*alias*’ formation is a common feature of podzolic fossil soil profiles in coastal dune deposits and on ocean beaches (Brookfield & Ahlbrandt, 1983; Pye & Tsoar, 2009). A similar indurated, brown-to-black coloured horizon is observed

along the present-day dune front of Le Pilat (Suchý *et al.*, 2013). The formation of this particular sandstone is related to rapid (less than 3000 years) cementation and induration processes affecting the aeolian sand deposits underlying a palaeosol within the dune barrier (Suchý *et al.*, 2013). The ‘garluche’ is a 0.3 to 0.4 m thick

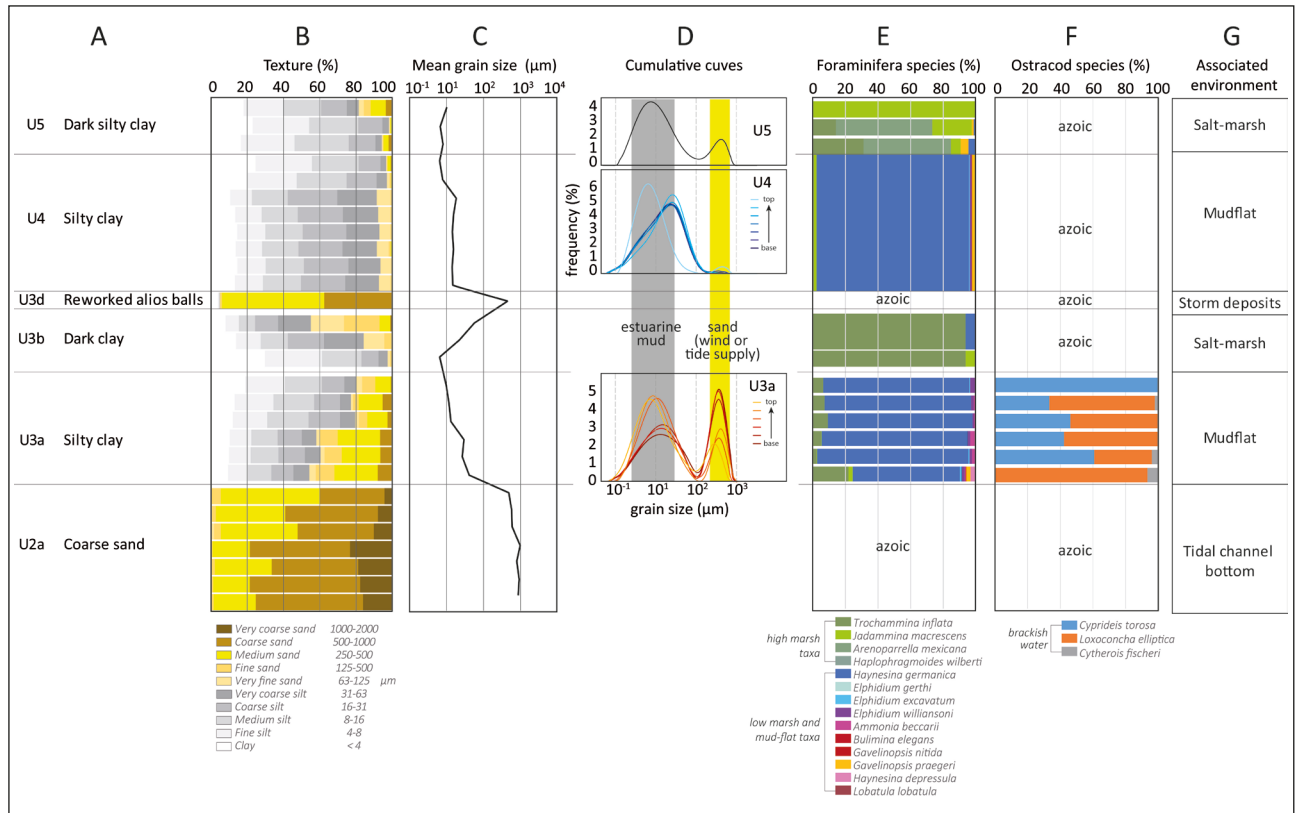


Fig. 10: Sedimentological analyses of stratigraphic units U1a to U5 obtained from sediment samples collected along the beach.

(A to D) Grain size characteristics. (E and F) Microfaunal content. (G) Coastal environments associated.

Fig. 10 : Analyses sédimentologiques des unités stratigraphiques U1 à U5 obtenues à partir des échantillons sédimentaires prélevés le long de la plage de l'Amélie. (A à D) Caractéristiques granulométriques. (E et F) Contenu micro-faunique. (G) Environnements côtiers associés.

bog iron hard-pan formed during the Holocene period within the upper Pleistocene ‘Sable des Landes’ sand formation, especially along small coastal streams or in swampy zones surrounding back-barrier freshwater lakes (Gourdon-Platel & Morin, 2004). Consequently, this deposit suggests the presence of a dune barrier in the vicinity of a swamp environment in the sector of La Glaneuse, in parallel with the development of a marsh environment on L’Amélie beach.

4.1.3.4 - Unit 3d

Unit 3d is a thin layer of reworked lithoclasts (we call ‘alias gravels’) with similar sedimentological characteristics to the alias sandstone (unit 3c). This layer was encountered close to the alias outcrop at an elevation of around +0.2 m asl. Here, the lithoclasts have a mean diameter up to 10 cm. A second layer of alias gravels was also observed in the central part of L’Amélie beach at an elevation of -1.4 m asl. The lithoclasts are smaller (mean diameter of 2 cm) and embedded in a clayey-silt sediment layer the top of which is characterized by a pavement of *Scrobicularia* shells (fig. 8e) dated to 3434-3070 cal. a BP (recalibrated date from Clavé, 2001). These field observations suggest a significant episode of dune barrier retreat leading to (i) the erosion of the alias formation and the transportation of the lithoclasts into the salt marsh environment by high-energy waves. The pavement of *Scrobicularia* shells is interpreted as an erosional surface.

4.1.4 - Unit 4: Second generation of estuarine mudflats (ca. 2700 to ca. 1250 cal. a BP)

Unit 4 is a clayey-silt deposit (mean grain size between 7 and 15 μm) covering a large spatial extent along the beaches of La Glaneuse and L’Amélie (fig. 7). The elevation of the sediment outcrops is between -1 and +1.3 m asl. Sediment samples collected at the base of the unit exhibit unimodal grain-size distribution curves (fig. 10d). The mode is around 25 μm reflecting a low-energy depositional environment. The foraminiferal assemblages are dominated by intertidal mudflat species with *Haynesina germanica* the dominant species (fig. 10e). These sedimentological characteristics indicate depositional conditions favourable to the formation of back-barrier estuarine mudflats after the erosion phase of unit 3d. The grain-size distribution curve of the sediment sample collected from the top of the unit shows a second mode around 400 μm (fig. 10d). The medium sand fraction represents 15 % of the total sediment volume reflecting episodic aeolian sand supplies from the dune front. This unit yields a high density of archaeological remains, especially wooden poles. On the archaeological site ALM-N008, a construction built on three rows of pine poles, preserved over 24.50 m in length and measuring 3 m in width, is dated to 2700-2495 cal. a BP (fig. 9b). Several tidal channels filled by organic-rich clayey-silt sediment containing a high density of oyster shells were observed in the field (fig. 8f). A radiocarbon age obtained on one of the oyster shells in life position

yielded an age of 1900-1510 cal. a BP (tab. 2). Several archaeological remains discovered within this deposit have been attributed to the Iron Age period, Antiquity and the Middle Ages (fig. 9e). The most recent archaeological evidence found in this mudflat sediment is a ceramic whose manufacture dates to the 7th century AD (site AML-N-006).

4.1.5 - Unit 5: Salt marshes (ca. 2500 to ca. 1070 cal. a BP)

Unit 5 is an organic-rich clayey-silt located in the northern and southern parts of L'Amélie beach at an elevation ranging from +0.7 to +1.8 m asl (fig. 7). The mean grain size is about 10 µm. The grain-size distribution is bimodal with a first mode at 8 µm and a second mode at 500 µm (fig. 10d). The sand fraction represents 15 % of the total sediment reflecting significant aeolian or tidal sediment supplies. The southern extent of the deposits shows numerous animal tracks on the surface (fig. 9f) and archaeological materials (lithic and ceramic). The foraminiferal content is dominated by *Jadammina macrescens*, with a few occurrences of *Haynesina germanica* and *Gavelinopsis praegeri* indicating a salt marsh environment. No radiocarbon age was obtained from this deposit, but ceramic fragments found on the archaeological site AML-N-002 were attributed to the Iron Age (ca. 2500-2400 cal. a BP). Consequently, unit 5 is contemporaneous with unit 4 in this section. The chrono-stratigraphical data from the dune section (see section 4.2) indicate that this deposit was buried by aeolian sand supplies from ca. 1370 cal. a BP onward.

On the northern part of L'Amélie beach, the salt marsh deposits display similar sedimentological characteristics. The foraminiferal assemblage is also dominated by a mixed low and high marsh taxa (fig. 10e). A radiocarbon sample obtained at the top of the unit gave an age of 1286-1070 cal. a BP (tab. 2). After this period, the salt marsh was buried by the coastal dune barrier.

4.2 - THE DUNE STRATIGRAPHY OF L'AMÉLIE BEACH

The dune stratigraphy was reconstructed from 28 sections described and topographically surveyed along the dune front of L'Amélie beach (fig. 7). The dune sequence is subdivided into five aeolian sands units (units 6 to 10) from the base to the top, separated by three layers of palaeosols or organic-rich sediment (figs. 11 & 12). The ages of the interbedded humic layers were obtained from seven radiocarbon ages (tab. 3).

4.2.1 - Unit 6: A dune slack environment (ca. 6180-5480 cal. a BP to ca. 1890-1370 cal. a BP)

Unit 6 is a 1.8 m thick gleyey sand overlying the L'Amélie sandstone (unit 1b) in the south of the L'Amélie dune front (between sections 18 and 28). The unit is encountered at an elevational range from +3.2 to +5 m asl. The material is very well sorted (mean sorting index of 0.42), symmetrically distributed (mean skewness values of -0.01) and very platykurtic (mean kurtosis index values of 0.32) medium sand (mean D50 of 325 µm) (fig. 12). These grain-size characteristics are consistent

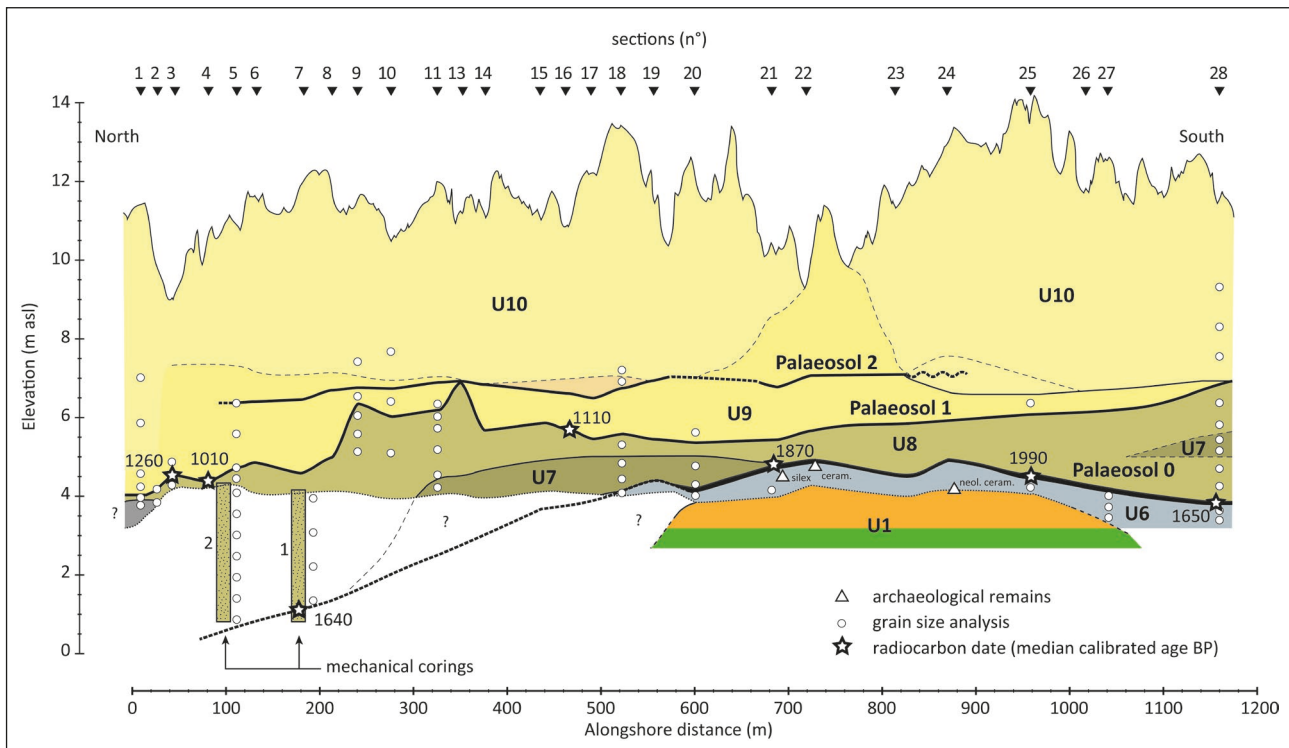


Fig. 11: Reconstructed dune stratigraphy along L'Amélie dune front.

The positions of sediment samples collected for sedimentological analyses and radiocarbon dating are also shown. Results of radiocarbon datings correspond to the median probability of calibrated ages.

Fig. 11 : Stratigraphie dunaire reconstituée le long du front de dune de l'Amélie. La position des échantillons sédimentaires prélevés pour les analyses géologiques et les datations est également indiquée. Les résultats des datations au radiocarbone correspondent à la probabilité médiane des âges calibrés.

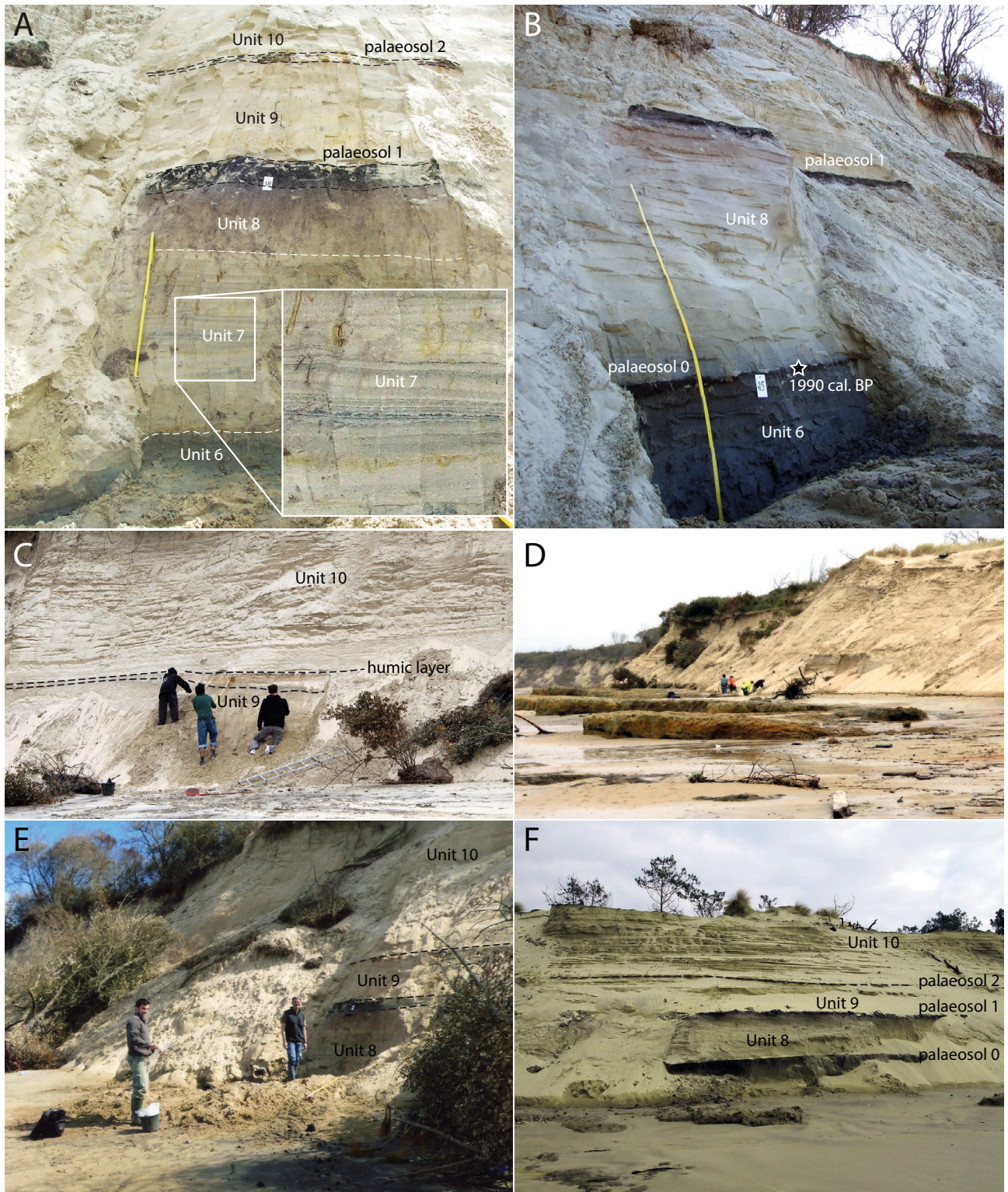


Fig. 12: Photographs illustrating the aeolian sand deposits along the dune front of L'Amélie beach.

(A) Section 18. (B) section 25. (C) section 14. (D) section 22. (E) section 9. (F) section 26.

Fig. 12 : Photographies illustrant les dépôts de sable éolien le long du front de dune de la plage de l'Amélie. (A) Section 18. (B) section 25. (C) section 14. (D) section 22. (E) section 9. (F) section 26.

with an aeolian origin. Stagnogley sands are frequently observed at the base of coastal sand deposits after a long period of dune stability (Packham & Willis, 1997). The process of gleyification suggests the stagnation of fresh water within permeable sediment during a long period of time as confirmed by the archaeological data and the radiocarbon dates obtained. The base of unit 6 is dated to the late Neolithic thanks to the archaeological

site AML-N-001 where a pit containing coal residues was excavated. A radiocarbon date obtained from a charcoal indicated an age of 5480-6180 cal. a BP (tab. 2). Within unit 6, numerous lithic and ceramic fragments have been dated to the Bronze Age, indicating that this deposit is contemporaneous with units 3. The top of unit 6 corresponds to a 0.1 to 0.2 m thick peaty palaeosol (palaeosol 0) containing a high proportion of

wood fragments which have yielded radiocarbon ages between 2150-1830 cal. a BP and 1890-1370 cal. a BP (tab. 3). This deposit can be interpreted as a dune slack environment where organic material accumulated in low-lying depressions between the dune ridges located several hundred metres seaward.

4.2.2 - Unit 7: Initial phase of dune invasion (1370-1890 cal. a BP to 1100-1340 cal. a BP)

Unit 7 is a 1 m-thick medium sand deposit observed between sections 11 and 21 at an elevation ranging from +4 to +5 m asl (fig. 11). To the south, the deposit buries palaeosol 0 indicating that this accumulation is younger than 1370-1890 cal. a BP. To the north, the unit dips northward under the surface of the upper beach. The sandy material is very well sorted (mean sorting index of 0.43), symmetrically distributed (mean skewness values of -0.03) and very platykurtic (mean kurtosis index values of 0.33) with a median grain size of around 333 µm suggesting an aeolian origin (fig. 13). The deposit is characterized by the presence of submillimetre thick horizontal stratification of silty sediment. Unit 7 corresponds to an initial deposit of aeolian sands on the southern edge of the estuarine salt marsh environment represented by units 4 and 5 (L'Amélie beach). Consequently, the silty stratification is interpreted as the episodic deposition of fine material during the highest astronomical tide flooding events.

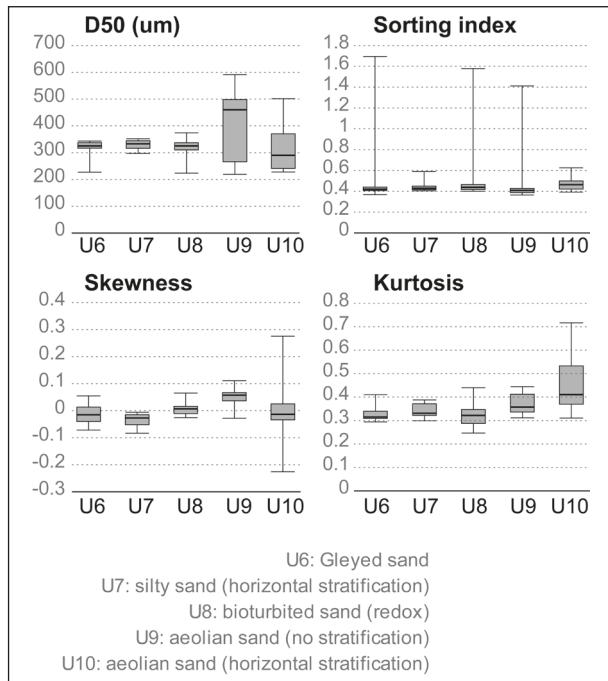


Fig. 13: Grain-size characteristics of the main stratigraphic units studied along L'Amélie dune front.

Fig. 13 : Caractéristiques granulométriques des principales unités stratigraphiques étudiées le long du front de dune de l'Amélie.

4.2.3 - Unit 8: Massive phase of dune invasion (1100-1340 to 800-1180 cal. a BP)

Unit 8 is observed along the entire dune front at an elevation ranging from +0.75 to +7 m asl with a thickness between 0.5 m (dune section 20) to 3.5 m (dune section 7, fig. 11). This deposit corresponds to a very well sorted

(mean sorting index of 0.44), symmetrically distributed (mean skewness values of 0.01) and very platykurtic (mean kurtosis index values of 0.32) medium sand (326 µm) (fig. 13). No internal stratification was noted because of bioturbation processes. Root penetration and microfaunal activity were evidenced by numerous rust-coloured stains related to redox conditions and attributed to phases of water saturation of aeolian sands. Along the longshore transect, unit 8 displays a slight north-south dip with a slope value of 0.25 %. This suggests northward dune progradation and a gradual burying of salt marsh sediments by aeolian sands. At the top of unit 8, a second 0.1 m thick palaeosol (palaeosol 1) is dated from 1100-1340 to 800-1180 cal. a BP (tab. 3).

4.2.4 - Unit 9: Dune invasion in a context of enhanced wind-forced aeolian activity (post-800-1180 cal. a BP)

Unit 9 is composed of aeolian medium to coarse sand (mean D50 of 461 µm) that is very well sorted (mean sorting index of 0.41), symmetrically distributed (mean skewness values of 0.06) and very platykurtic (mean kurtosis index values of 0.36) (fig. 13). The elevation ranges from +4.5 to +7 m asl (fig. 11). The deposit thickens northwards. No internal stratification was observed, but we noted a subhorizontal humic horizon at 7 m asl, indicating a short period of dune stability. This sediment unit is characterized by a significant proportion of coarse sands. The size fraction between 500 and 1000 µm accounts for 25 % of the sediment. This is interpreted as an increase in the windiness and/or storminess associated with the cooler climate of the Little Ice Age.

4.2.5 - Unit 10: Modern aeolian sand dune

Unit 10 is a 5 m thick deposit of medium aeolian sand (290 µm) that is very well sorted (mean sorting index of 0.46), symmetrically distributed (mean skewness values of -0.01) and very platykurtic (mean kurtosis index values of 0.41). Along the dune front, horizontal stratifications were observed (fig. 12). Despite the absence of information about the internal orientation of the strata, these features are similar to those of established foredunes (Hesp, 1988) and are produced by sand deposition within increasing vegetation cover on relatively gentle near-horizontal slopes.

5 - DISCUSSION

5.1 - NEW SEDIMENTOLOGICAL AND ARCHAEOLOGICAL RECORDS OF THE HOLOCENE RSL RISE

The history of the Holocene Relative Sea Level (RSL) along the Aquitaine coast is poorly known. Using a Glacial Isostatic Adjustment (GIA) model, Lambeck (1997) proposed a first RSL curve for the locality of Royan. However, the model used is constrained by very limited RSL data. Pontee *et al.* (1998) suggest RSL fluctuated around the present-day level in the Gironde

area over the last 4000 years in a series of low-amplitude (<1 m) positive and negative trends. Recently, Stephan and Goslin (2014) followed by García-Artola *et al.* (2018) have used sedimentological and stratigraphic data collected by many authors from the salt marshes of Charentes and Gironde (Gabet, 1973; Ters, 1973; Visset *et al.*, 1989, 1990; Bourgueil 1995, 2005; Diot & Tastet 1995; Tastet *et al.*, 2000a,b; Clavé *et al.*, 2001 ; Wang *et al.*, 2006) to produce a series of 11 index points, six marine limiting ages, and two freshwater limiting ages (tab. 4, fig. 14). Data were then fitted to a spatio-temporal empirical hierarchical model (Cressie & Wikle, 2011; Kopp *et al.*, 2016; Ashe *et al.*, 2019) to propose an RSL curve with 1σ and 2σ confidence interval envelopes (García-Artola *et al.*, 2018) for the SW France coastal area. The oldest freshwater limiting date constrains RSL to below -13.1 ± 2.6 m at ca. 9000 cal. a BP. Two marine limiting dates place RSL above -11.1 ± 2.6 m at ca. 8500 cal. a BP and above -9.5 ± 2.6 m at ca. 8100 cal. a BP. The oldest SLIP indicates RSL was at -5.2 ± 2.9 m at ca. 7300 cal. a BP. RSL rose to -3.5 ± 2.9 m at ca. 7100 cal. a BP. Then, RSL rose from -3.0 ± 2.9 m at ca. 6500 cal. a BP to -1.5 ± 2.6 m at ca. 4700 cal. a BP at a rate of 0.7 ± 0.5 mm.yr $^{-1}$. The late Holocene is only constrained by three index points that place RSL at ca. -1.0 ± 2.5 m at ca. 2900 cal. a BP and at 0.5 ± 2.8 m at 600 cal. a BP. SLIPs produced in this paper are consistent with previous RSL records and provide two new RSL records for the last 3000 years.

5.2 - PALAEOGEOGRAPHIC CHANGES OF THE GIRONDE MOUTH

Most of the sedimentary outcrops identified on the L'Amélie and La Glaneuse beaches correspond to Holocene estuarine mud-flat and salt marsh deposits accumulated within a large topographic depression of

Pleistocene age. The fine estuarine sediments (units 3 to 5) cover a deposit of coarse sand (unit 2a) attributed to a tidal channel that could correspond to the 'Soulac channel' indicated in several palaeogeographic reconstructions of the Gironde estuarine mouth (Allen *et al.*, 1974; Pontee *et al.*, 1998). In agreement with the palaeogeographical maps of the North Médoc peninsula produced by Pontee *et al.* (1998), these results provide a more detailed view of Holocene coastal changes with better chronological resolution in the areas of L'Amélie and La Glaneuse beaches. The presence of a coastal marsh open to the east and connected to the mouth of the Gironde starting at 6000 BP is confirmed by this study. According to Pontee *et al.* (1998), the salt marsh was bordered on its western side by a coastal dune complex with a coastline located further west than at the present-day. The formation of this first coastal dune barrier is not well-dated, but the oldest palaeosol-date in the Médoc (Montalivet) is 6170-5610 cal. a BP (Dubreuilh, 1971). Multiple younger palaeosols are known with ages ranging from 4000 to 3000 cal. a BP along the Médoc coastline (Tastet & Pontee, 1998), as are multiple periods of aeolian activity and dune fixation (Clarke *et al.*, 2002). We assume the dark sandstone ('aliots' or 'garluche') which crops out on La Glaneuse beach is contemporary with one of these two periods and could correspond to the inner part of a first coastal dune complex. Suchý *et al.* (2013) recently studied the black sandstone horizon forming the base of the Dune du Pilat, 100 km south of the study area. They provided insight into the composition and the formation processes of organic cements and provided information on the rates at which cementation and induration occur in these temperate-climate coastal deposits. An initial aeolian sand deposit was impregnated by an amorphous substance rich in organic matter and of humate composition derived from a palaeosol (palaeosol 1). The humate formed thin coats on the grain surfaces and grain contacts, thus cementing

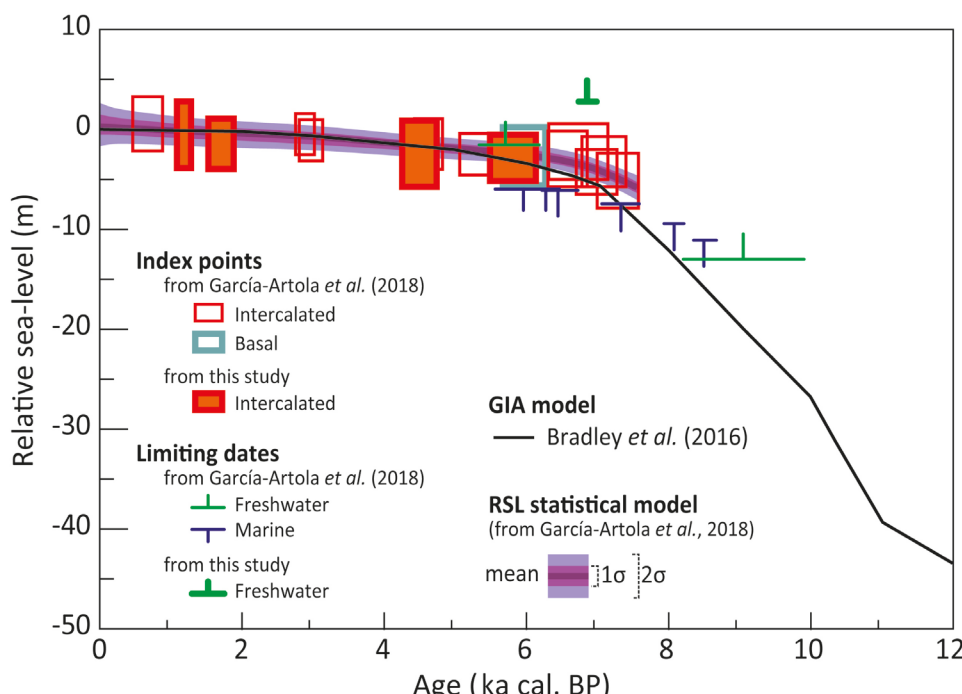


Fig. 14: RSL records produced in this study.

Data are plotted on observations produced by García-Artola *et al.* (2018) and compared to GIA and spatio-temporal statistical model predictions for the Charentes and Aquitaine coastal regions of France.

*Fig. 14 : Enregistrements du niveau marin relatif produits dans cette étude. Les données sont tracées sur les observations produites par García-Artola *et al.* (2018) et comparées au modèle prédictif d'ajustement glacio-isostatique et au modèle statistique spatio-temporel pour les côtes françaises de Charentes et d'Aquitaine.*

Unique sample ID	Reference	Region code	Sub-region	Latitude	Longitude	Dating method	Corrected age (${}^{\circ}\text{C}$ à BP)	Age 2 σ Uncertainty + (cal a)	Age 2 σ Uncertainty - (cal a)	Sample depth/overburden thickness (m)	Depth to consolidated substrate (m)	Sample elevation uncertainty + (m)	Type	Primary indicator type	Secondary indicator type	Supporting evidence	Sample indicative meaning	RSL (m)	RSL 2 σ Uncertainty + (m)	RSL 2 σ Uncertainty - (m)			
FR 173	Visset et al. 1989; Stéphan & Goslin 2014 (as in García-Artola et al. 2018)	4	Coast of Charentes, France	46.45	-0.844	1	5200	122	5974	300	310	4.775	nd	-1.37	2.55	0	5	Undifferentiated salt marsh environment	5	HAT-MTL	-2.696	3.03	3.03
FR 174	Visset et al. 1990; Stéphan & Goslin 2014 (as in García-Artola et al. 2018)	4	Coast of Charentes, France	46.378	-0.75	1	6830	120	7349	237	264	9.35	nd	-7.85	2.55	2.55	5	Marine limiting	9	MTL	-7.535	2.55	2.55
FR 175	Visset et al. 1990; Stéphan & Goslin 2014 (as in García-Artola et al. 2018)	4	Coast of Charentes, France	46.378	-0.75	1	6010	110	6444	270	247	7.95	nd	-6.45	2.55	2.55	5	Marine limiting	9	MTL	-6.135	2.55	2.55
FR 176	Allard et al. 2008; Stéphan & Goslin 2014 (as in García-Artola et al. 2018)	4	Coast of Charentes, France	45.943	-1.14	1	8030	50	8495	176	145	4.1	nd	-11.42	2.60	2.60	5	Marine limiting	9	MTL	-11.132	2.60	2.60
FR 177	Allard et al. 2008; Stéphan & Goslin 2014 (as in García-Artola et al. 2018)	4	Coast of Charentes, France	45.943	-1.14	1	7610	40	8076	137	142	2.45	nd	-9.77	2.60	2.60	5	Undifferentiated salt marsh environment	13	HAT-MTL	0.524	2.83	2.83
FR 178	Ters 1973; Stéphan & Goslin 2014 (as in García-Artola et al. 2018)	4	Coast of Charentes, France	45.845	-1.062	1	642.990	111	617	274	143	nd	nd	1.74	2.41	0	5	Undifferentiated salt marsh environment	5	HAT-MTL	-1.454	2.61	2.61
FR 179	Clavé et al. 2001; Stéphan & Goslin 2014 (as in García-Artola et al. 2018)	4	Coast of Charentes, France	45.905	-1.295	1	4140	70	4674	167	228	0.94	nd	-0.19	2.19	0	5	Undifferentiated salt marsh environment	7	MTL to -1m	-0.576	2.26	2.26
FR 180	Clavé et al. 2001; Stéphan & Goslin 2014 (as in García-Artola et al. 2018)	4	Coast of Charentes, France	45.905	-1.295	1	3080	40	2863	167	131	2.9	nd	-1.23	2.18	0	5	Inner or semi-enclosed lagoon	7	MTL to -1m	-0.576	2.26	2.26
FR 181	Gabet 1973; Stéphan & Goslin 2014 (as in García-Artola et al. 2018)	4	Coast of Charentes, France	45.905	-1.295	1	4952.990	162	5704	467	389	0.4	nd	-1.72	2.20	2.19	1	Freshwater limiting	12	MTL	-1.566	2.20	2.19
FR 182	Bourguill 1995; Bourguill 2005; Stéphan & Goslin 2014 (as in García-Artola et al. 2018)	4	Coast of Charentes, France	46.024	-0.892	1	8140	345	9055	843	16.085	nd	-13.41	2.60	2.60	1	Freshwater limiting	13	MTL	-13.117	2.60	2.60	
FR 183	Wang et al. 2006; Stéphan & Goslin 2014 (as in García-Artola et al. 2018)	4	Coast of Charentes, France	45.518	-0.854	1	2840	70	2960	196	171	2.55	nd	0.14	2.13	0	5	Undifferentiated salt marsh environment	4	HAT-MTL	-1.097	2.51	2.51
FR 184	Wang et al. 2006; Stéphan & Goslin 2014 (as in García-Artola et al. 2018)	4	Coast of Charentes, France	45.518	-0.854	1	5560	190	5960	424	400	8.8	nd	-6.11	2.13	2.13	5	Marine limiting	9	MTL	-6.014	2.13	2.13
FR 185	Wang et al. 2006; Stéphan & Goslin 2014 (as in García-Artola et al. 2018)	4	Coast of Charentes, France	45.518	-0.854	1	5480	100	6272	190	273	8.8	nd	-6.11	2.13	2.13	5	Marine limiting	9	MTL	-6.014	2.13	2.13
FR 186	Tastet et al. 2000b; Stéphan & Goslin 2014 (as in García-Artola et al. 2018)	4	Coast of Charentes, France	45.518	-0.854	1	4640	100	5364	223	318	3.16	nd	-0.47	2.13	2.13	0	High marsh environment	1	HAT-MHW	-2.526	2.19	2.19
FR 187	Tastet et al. 2000b; Stéphan & Goslin 2014 (as in García-Artola et al. 2018)	4	Coast of Charentes, France	45.518	-0.854	1	6130	130	7014	278	336	5.175	nd	-3.49	2.13	2.13	0	Low marsh environment	3	MHW-MTL	-4.207	2.28	2.28
FR 188	Tastet et al. 2000a; Stéphan & Goslin 2014 (as in García-Artola et al. 2018)	4	Coast of Charentes, France	45.272	-0.811	1	6210	128	7099	316	303	1.725	nd	-2.10	2.48	2.48	0	Undifferentiated salt marsh environment	5	HAT-MTL	-3.487	2.89	2.89
FR 189	Tastet et al. 2000a; Stéphan & Goslin 2014 (as in García-Artola et al. 2018)	4	Coast of Charentes, France	45.279	-0.847	1	5893	181	6729	434	410	1.5	nd	-0.87	2.48	2.48	0	Undifferentiated salt marsh environment	5	HAT-MTL	-2.262	2.89	2.89
FR 190	Tastet et al. 2000a; Stéphan & Goslin 2014 (as in García-Artola et al. 2018)	4	Coast of Charentes, France	45.281	-0.852	1	5730	128	6536	305	251	3.205	nd	-1.58	2.48	2.48	0	Undifferentiated salt marsh environment	5	HAT-MTL	-2.967	2.89	2.89
FR 191	Tastet et al. 2000a; Stéphan & Goslin 2014 (as in García-Artola et al. 2018)	4	Coast of Charentes, France	45.281	-0.852	1	6430	141	7338	241	331	5.475	nd	-3.85	2.48	2.48	0	Undifferentiated salt marsh environment	5	HAT-MTL	-5.237	2.89	2.89
FR 192	this study	4	Coast of Charentes, France	45.502	-1.139	1	1260	50	1203	83	133	0	nd	1.34	2.13	2.13	0	Undifferentiated salt marsh environment	4	HAT-MTL	-0.567	3.33	3.33
FR 193	this study	4	Coast of Charentes, France	45.498	-1.142	1	2108	74	1701	196	191	0	nd	-0.08	2.13	2.13	0	Low marsh environment	3	MHW-MTL	-1.472	2.62	2.62
FR 194	this study	4	Coast of Charentes, France	45.503	-1.139	1	3984	70	4455	347	219	0	nd	-0.53	2.14	2.14	0	Undifferentiated salt marsh environment	4	HAT-MTL	-2.433	3.34	3.34
FR 195	this study	4	Coast of Charentes, France	45.491	-1.146	1	5040	130	5790	386	308	0	nd	3.35	0.26	0.26	1	Freshwater limiting	13	MTL	2.779	2.13	2.13
FR 196	this study	4	Coast of Charentes, France	45.502	-1.139	1	6025	50	6869	127	127	1.95	nd	-0.23	2.14	2.14	0	High marsh environment	1	HAT-MHW	-2.906	2.37	2.37

Tab. 4 : Excerpt from the RSL database for the Atlantic coasts of Europe (García-Artola et al., 2018) limited to sub-region 7 corresponding to the coast of Charentes and supplement by RSL data produced in this study.

Tab. 4 : Extrait de la base de données des niveaux marins relatifs pour les côtes atlantiques de l'Europe (García-Artola et al., 2018) limitée à la sous-région n°7 correspondant à la côte des Charentes et complétée par les données RSL produites dans cette étude.

the sediment and causing its penetrative black colouring. The induration of the sand was completed over a relatively short period (less than 3500 years). A similar geochemical process, frequently encountered at the interface between sand dune swamps and stagnant lakes (Lapen & Wang 1999; Gourdon-Platel & Morin 2004), could explain the presence of the dark sandstone on La Glaneuse beach.

The sedimentary infilling reconstructed along the beaches under study shows two main stages of estuarine deposition, interrupted by a major episode of marine erosion (figs. 15 & 16). This erosional event is characterized by an abrupt change in hydrodynamic conditions inside the estuarine marsh, as proved by the

abundant production of blackened sandstone pebbles. These lithoclasts were eroded from the nearby source bed in the north of the study area, rounded by wave action, and transported and incorporated into estuarine sediments further south. In the median part of L'Amélie beach, these sandstone pebbles are interbedded into a layer of dark clay containing abundant shells of *Scrobicularia*. The radiocarbon date obtained from one of these shells gave an age of 3070-3435 cal. a BP (Clavé, 2001; tab. 2).

Again, these results are broadly consistent with the geological surveys conducted in the inner part of the mouth of the Gironde where two main stages of salt marsh sedimentary infilling were recognized. The first generation of marshes is separated from the second by

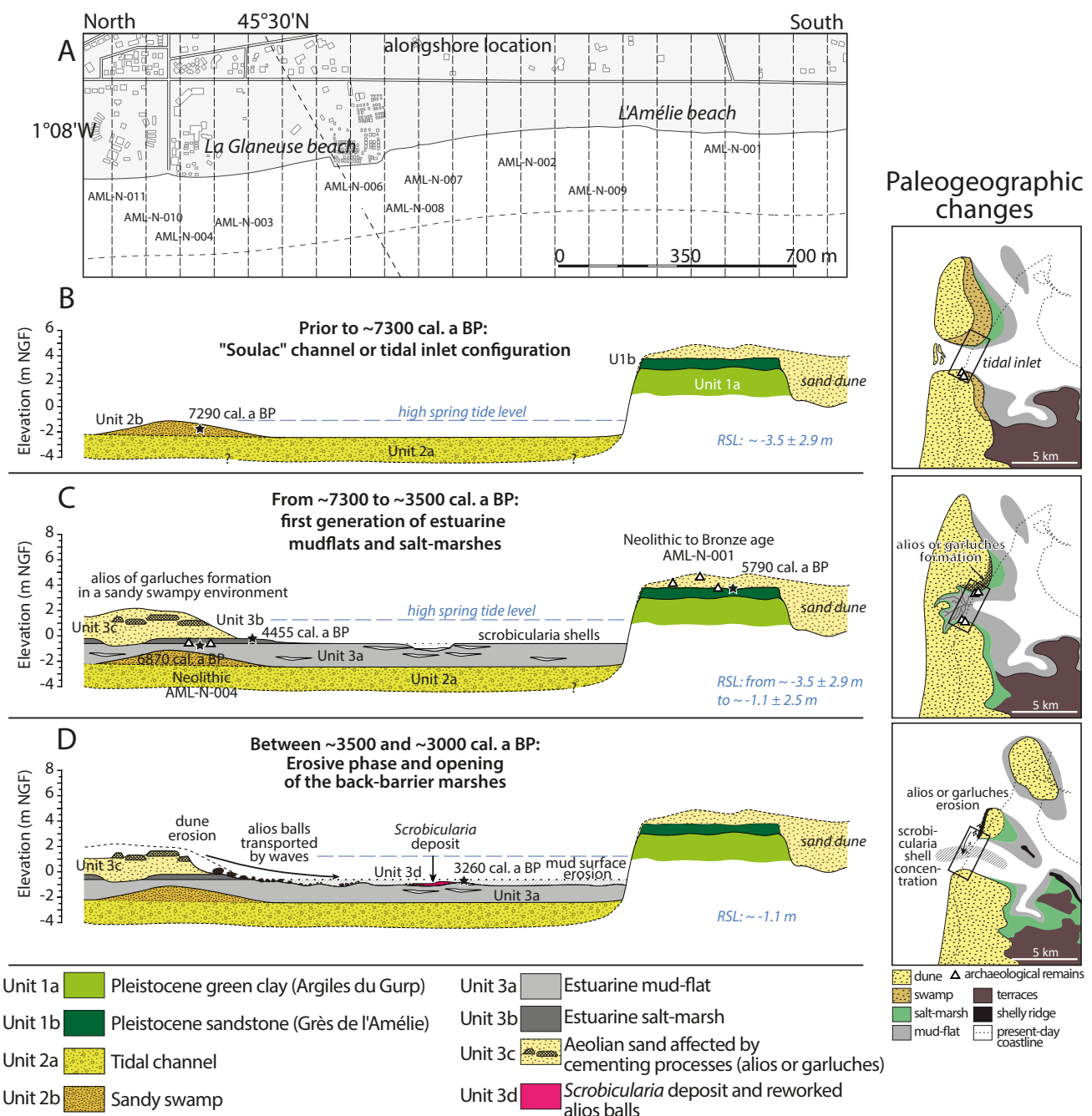


Fig. 15: Mid-Holocene sedimentary filling sequence of L'Amélie beach and interpretation of associated palaeogeographic changes from ca. 7000 to 3000 cal. a BP.

Fig. 15 : Séquence de remplissage sédimentaire de la plage de l'Amélie et interprétation des changements paléogéographiques associés depuis environ 7000 jusqu'à 3000 a cal. BP.

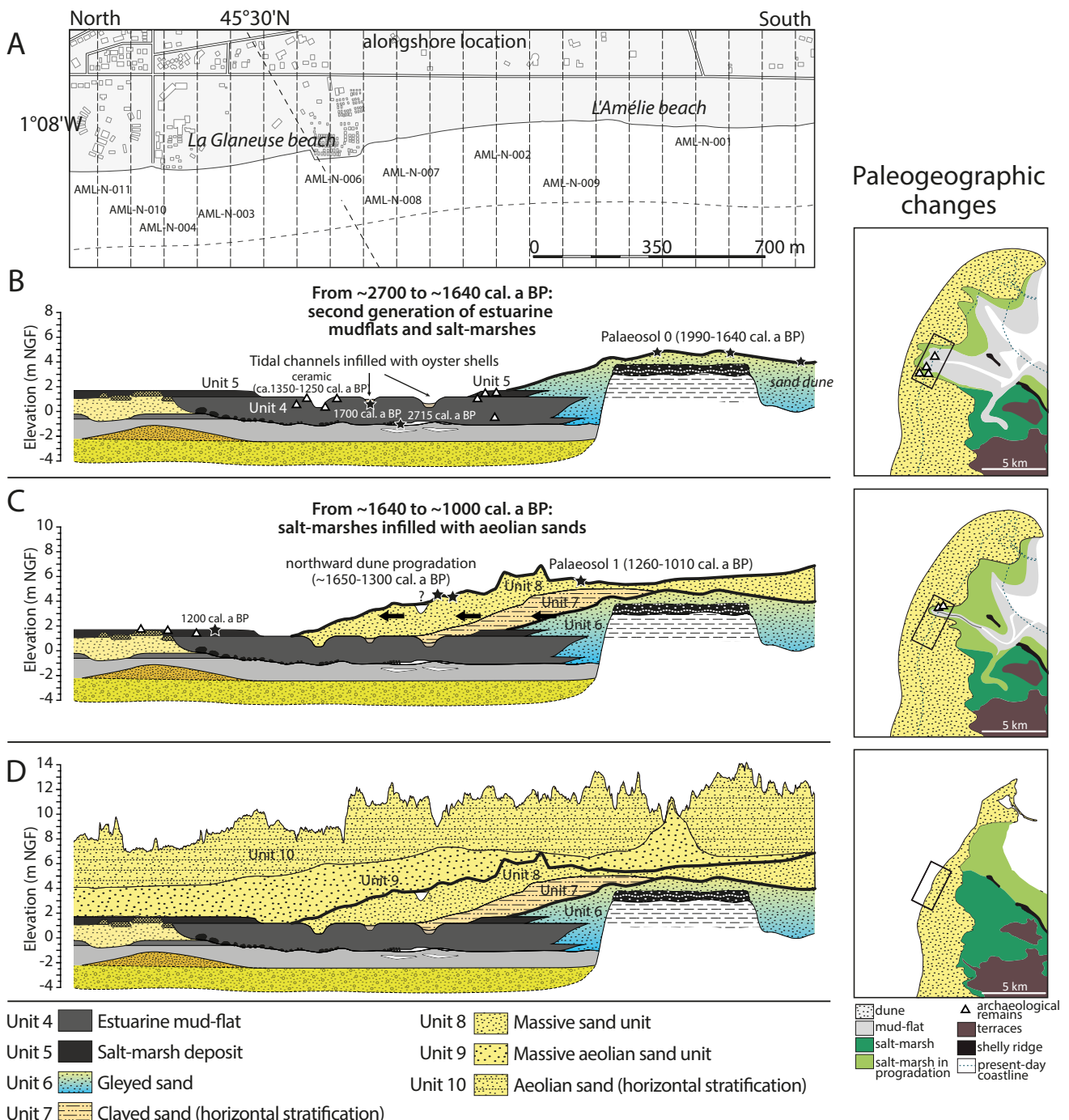


Fig. 16: Mid to late Holocene sedimentary filling sequence of L'Amélie beach/dune system and interpretation of associated palaeogeographic changes from ca. 3000 cal. a BP to the present-day.

Fig. 16 : Séquence de remplissage sédimentaire de la plage de l'Amélie et de formation des dunes, interprétation des changements paléogéographiques associés depuis environ 3000 a cal. BP jusqu'à aujourd'hui.

the ‘Cordon de Richard’ shelly ridge, the construction of which was interpreted as the result of a sea-level rise and/or increase in storminess (Pontee *et al.*, 1998; Massé *et al.*, 2001; Clavé, 2001). Radiocarbon ages from *Scrobicularia* shells collected along the shelly ridge over a long time period ranging from 3175 to 2110 cal. a BP (Massé *et al.*, 2001) while the age obtained on L'Amélie beach indicates a slightly more ancient age for coastal changes of around 3450-3090 cal. a BP. The period around 3000-2700 cal. a BP has been widely recognized as a period of climate deterioration in NW Europe (Van Geel *et al.*, 1996; Barber *et al.*, 2003, 2004; Magny, 2004; Dark

2006; Gandouin *et al.*, 2009; Charman, 2010; Swindles *et al.*, 2013; Tisdall *et al.*, 2013), characterized by colder and wetter climatic conditions with increased rainfall and largely enhanced storminess (Van Geel *et al.*, 1996; Clarke & Rendell, 2009). Major disruptions of coastal sedimentary environments were also identified all along the European coasts, either in the English Channel region (Long & Hughes, 1995; Billeaud *et al.*, 2009; Sorrel *et al.*, 2009; Lespez *et al.*, 2010; Tessier *et al.*, 2012) or along the Atlantic coasts (Pontee *et al.*, 1998; Tastet & Pontee, 1998; Clavé *et al.*, 2001; Moura *et al.*, 2007; Sorrel *et al.*, 2009; Allard *et al.*, 2009; Stéphan *et al.*, 2015).

5.3 - PERIODS OF DUNE STABILITY AND AEOLIAN SAND DRIFT EPISODES

Many attempts have been made to find a common chronological framework for aeolian sand activity/stability phases along the Aquitaine coast. Two well-differentiated records were used: humic sand units or palaeosols dated using radiocarbon (Froidefond & Legigan, 1985; Tastet, 1998; Dubreuilh, 1971; Tastet & Pontee, 1998) and aeolian sand units dated using luminescence measurements (IRSL) (Tastet, 1998; Clarke *et al.*, 1999, 2002; Sitzia *et al.*, 2015). The two methods appear complementary. The IRSL measurements on sands yield an age at which sand was buried, and underwent no reworking. The measurement therefore provides information about the last phase of wind activity at a given location. Radiocarbon dating of palaeosols provides information about the dune surface fixation over a variable time period and at a given location. Several palaeosols are found in succession in the stratigraphy and may indicate phases of stability separated by phases of sand invasion. However, the organic layers can also be eroded by wind so that the absence of palaeosols within a stratigraphy does not mean that the dunes were never stable. In addition, the ages obtained are only partial and do not provide very accurate information. Indeed, the problems of carbon pollution within organic layers usually require consideration of the total organic material (bulk). The age obtained cannot be used to define the beginning and end of the period of stability. These time

limits can only be approached statistically by multiplying the radiocarbon dating of each palaeosol.

Thanks to the topographic survey of palaeosols and several radiocarbon ages obtained along the 1 km dune front of L'Amélie beach, the chronostratigraphy of the coastal dune system is locally well-reconstructed. If we consider only the median probability of radiocarbon calibrated ages, two main periods of dune stability are recognized: (i) from 1990 to 1640 cal. a BP (palaeosol 0), (ii) from 1260 to 1010 cal. a BP (palaeosol 1). These periods were interrupted by phases of aeolian sand invasion burying the salt marsh deposits dated from 1640 to 1250 cal. a BP (stratigraphic units 7 and 8) and after 1250 cal. a BP (stratigraphic units 9 and 10). A shorter third period of stability is also represented by a thin humic layer between stratigraphic units 9 and 10. Because of the high proportion of coarse sand in the aeolian sediment, unit 9 is interpreted as evidence of stronger winds. In NW Europe, several periods of coastal sand drift were recorded over the last 1000 years especially during the cool 'Little Ice Age' (ca. 450-150 a e & Rendell, 2009; Lamb & Frydendahl, 2005; Costas *et al.*, 2012; Danielsen *et al.*, 2012; Van Vliet-Lanoë *et al.*, 2014) in a context of increased storminess. Despite the lack of chronological information, we hypothesize that unit 9 is dated to the LIA period, while unit 10 formed over the last centuries before the dunes were artificially fixed with pine forest (Buffault, 1942).

In Figure 17 and Table 5, the periods of dune stability recognized along the L'Amélie dune front are compared

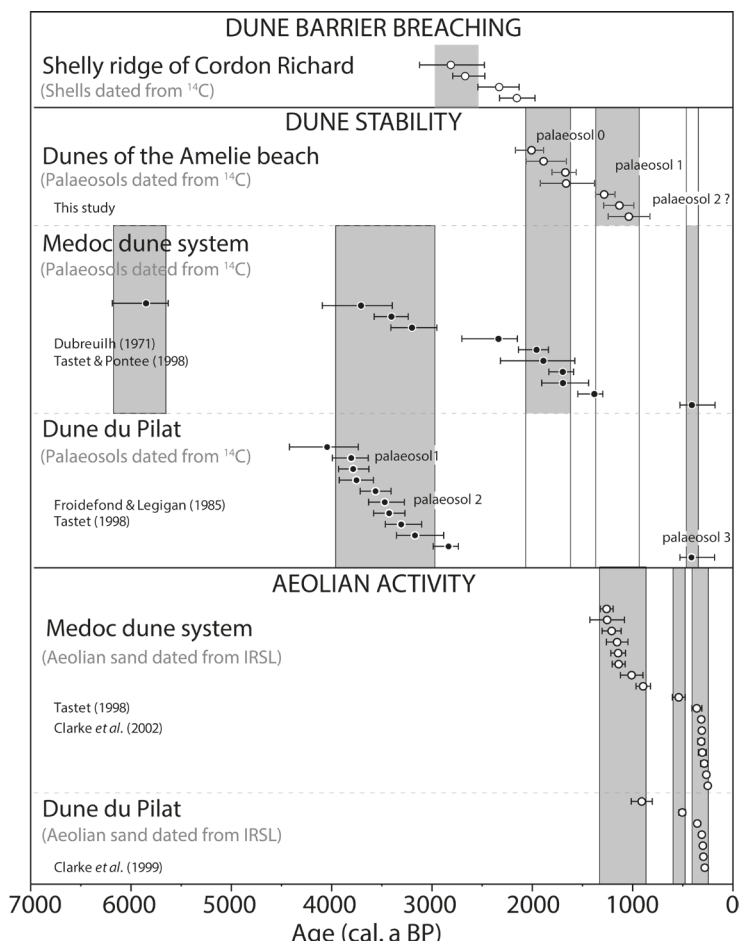


Fig. 17: Synthesis of the data available along the Aquitaine coast related to the chronology of the coastal dunes.

The middle gray bands correspond to the periods of stability of the coastal dunes defined from the radiocarbon dating of the peat layers. The data presented in this paper are compared with previously published data (Froidefond & Legigan, 1985; Tastet, 1998; Dubreuilh, 1971; Tastet & Pontee, 1998) which have been calibrated from the IntCal13 curve (Reimer *et al.* 2013) using Calib 7.0 software (Stuiver & Reimer, 1993). The lower gray bands correspond to the phases of wind activity and mobility of the sand bodies defined from the IRSL dating performed on the quartz grains (Clarke *et al.*, 2002; Tastet, 1998; Clarke *et al.* 1999). The radiocarbon data relative to the formation of the "cordon de Richard" shelly ridge (Gironde estuary) are also indicated. These data were calibrated by the procedure described in section 3.3.

*Fig. 17 : Synthèse des données disponibles le long de la côte Aquitaine relative à la chronologie dunaire. Les zones vertes centrales correspondent aux périodes de stabilité des dunes définies à partir de la datation par le radiocarbone des niveaux de paléosols tourbeux. Les données présentées dans ce papier sont comparées aux données antérieurement publiées (Froidefond & Legigan, 1985 ; Tastet, 1998 ; Dubreuilh, 1971 ; Tastet & Pontee, 1998) qui ont été calibrées à partir de la courbe IntCal13 (Reimer *et al.*, 2013) avec le logiciel Calib 7.0 (Stuiver & Reimer 1993). Les bandes grises inférieures correspondent aux phases d'activité éoliennes et de mobilité des corps sableux connues à partir de la datation par IRSL effectuées sur les grains de quartz éoliens (Clarke *et al.*, 2002 ; Tastet, 1998 ; Clarke *et al.*, 1999). Les données de datation radiocarbone relatives à la formation du cordon de Richard (estuaire de la Gironde) sont également indiquées. Ces données ont été calibrées en suivant la même procédure décrite à la section 3.3.*

	References	Method	Age BP	Age cal. a BP		Field reference	Sample type	Lab. Reference	Coord. WGS84		Locality
				min. (med.) max.	min. (med.) max.				Lat. N	long. E	
Dunes of Medoc											
stability phases	Tastet & Pontee (1998)	¹⁴ C	310 ±60	502 (384) 153	1448 (1566) 1797	HO9210 (core)	Organic sand under a barchan dune	Beta 95393	45.372	-1.124	Montalivet
	Tastet & Pontee (1998)	¹⁴ C	1450 ±70	1523 (1357) 1273	427 (593) 677	Montalivet	Stump in life position	UQ2147	45.366	-1.160	Montalivet
	Dubreuilh (1971)	¹⁴ C	1750 ±100	1884 (1671) 1415	66 (279) 535	Lede des Frayres niv.20	grey humic sands	*	45.327	-1.160	Montalivet
	Tastet & Pontee (1998)	¹⁴ C	1760 ±50	1813 (1672) 1564	137 (278) 386	TM 96056	Wood in palaeosol between sand layers	Beta 102697	45.481	-1.153	Amélie beach, Soulac
	Tastet & Pontee (1998)	¹⁴ C	1920 ±130	2296 (1866) 1552	-346 (84) 398	La Barrière	Peat between sand layers	UQ 1990	45.321	-1.159	Montalivet
	Tastet & Pontee (1998)	¹⁴ C	1980 ±60	2115 (1935) 1816	-165 (15) 134	Gurp Niv.2	Wood above the clay of the Gurp	LY 4597	45.452	-1.154	Négade beach, Soulac
	Dubreuilh (1971)	¹⁴ C	2300 ±70	2681 (2315) 2126	-731 (-365) -176	Dépé niv.20	Black peat	*	45.417	-1.159	Grayan beach
	Dubreuilh (1971)	¹⁴ C	3000 ±90	3388 (3177) 2929	-1438 (-1227) -979	Dépé niv.18	Peat with debris roots	*	45.417	-1.159	Grayan beach
	Tastet & Pontee (1998)	¹⁴ C	3160 ±60	3555 (3383) 3216	-1605 (-1433) -1266	TM 96049	Sandy peat between sand layers	Beta 95383	45.386	-1.159	Montalivet
	Tastet & Pontee (1998)	¹⁴ C	3420 ±135	4074 (3687) 3374	-2124 (-1737) -1424	Euronat niv. 4	Peat between sand layers	UQ 1991	45.416	-1.159	Euronat. Beach, Grayan
	Dubreuilh (1971)	¹⁴ C	5100 ±90	6169 (5832) 5611	-4219 (-3882) -3661	Saint-Nicolas niv.14	Peat	*	45.298	-1.162	Montalivet
activity phases	Clarke et al. (2002)	IRSL	275 ±50	250 (225) 200	1700 (1725) 1750	Lettres des Joncs	aeolian sand, crescentic ridge	SG6	44.442	-1.217	Lettres des Joncs
	Clarke et al. (2002)	IRSL	290 ±60	270 (240) 210	1680 (1710) 1740	Lettres des Joncs	aeolian sand, crescentic ridge	SG7	44.433	-1.224	Lettres des Joncs
	Clarke et al. (2002)	IRSL	310 ±75	298 (260) 223	1653 (1690) 1728	Piquerot	aeolian sand, barchan	HT4	45.202	-1.141	Piquerot
	Tastet (1998)	IRSL	325 ±40	320 (280) 240	1630 (1670) 1710	Mourey (east)	aeolian sand, barchanoid ridge	NM 3	45.322	-1.124	Dunes of Grayan
	Tastet (1998)	IRSL	335 ±35	325 (290) 255	1625 (1660) 1695	La Gastouse (east)	aeolian sand, isolated parabolic dune	NM 5	45.442	-1.139	Dunes of Grayan
	Clarke et al. (2002)	IRSL	335 ±50	310 (285) 260	1640 (1665) 1690	St. Nicolas	aeolian sand, parabolic dune	HT6	45.312	-1.128	St. Nicolas
	Clarke et al. (2002)	IRSL	340 ±40	310 (290) 270	1640 (1660) 1680	Ginestras	aeolian sand, crescentic ridge	HT5	45.309	-1.140	Ginestras
	Tastet (1998)	IRSL	380 ±50	385 (335) 285	1565 (1615) 1665	Labiau (west)	aeolian sand, isolated barchan	NM 7	45.433	-1.114	Dunes of Grayan
	Tastet (1998)	IRSL	560 ±65	580 (515) 450	1370 (1435) 1500	Mourey (west)	aeolian sand, barchan	NM 1	45.324	-1.130	Dunes of Grayan
	Clarke et al. (2002)	IRSL	920 ±145	943 (870) 798	1008 (1080) 1153	Miqueou	aeolian sand, parabolic dune	SG3	44.413	-1.189	Miqueou
	Clarke et al. (2002)	IRSL	1035 ±225	1098 (985) 873	853 (965) 1078	Piquerot	aeolian sand, parabolic dune	HT2	45.198	-1.128	Piquerot
	Clarke et al. (2002)	IRSL	1165 ±130	1180 (1115) 1050	770 (835) 900	Lartigues	aeolian sand, parabolic dune	SG1	44.407	-1.185	Lartigues
	Clarke et al. (2002)	IRSL	1170 ±145	1193 (1120) 1048	758 (830) 903	Piquerot	aeolian sand, parabolic dune	HT1	45.199	-1.128	Piquerot
	Clarke et al. (2002)	IRSL	1180 ±215	1238 (1130) 1023	713 (820) 928	Ispe	aeolian sand, parabolic dune	SG5	44.441	-1.196	Ispe
	Clarke et al. (2002)	IRSL	1235 ±190	1280 (1185) 1090	670 (765) 860	Miqueou	aeolian sand, parabolic dune	SG4	44.414	-1.193	Miqueou
	Clarke et al. (2002)	IRSL	1280 ±345	1403 (1230) 1058	548 (720) 893	Piquerot	aeolian sand, parabolic dune	HT3	45.205	-1.128	Piquerot
	Clarke et al. (2002)	IRSL	1285 ±130	1300 (1235) 1170	650 (715) 780	Lartigues	aeolian sand, parabolic dune	SG2	44.407	-1.188	Lartigues
Amelie frontdune											
stability phases	This study	¹⁴ C	1090 ±70	1220 (1014) 803	730 (936) 1147	Amelie beach	Palaeosol 1 (section 4) wood	VERA-51335	45.497	-1.142	Amélie beach, Soulac
	This study	¹⁴ C	1180 ±70	1264 (1108) 963	686 (842) 987	Amelie beach	Palaeosol 1 (section 16)	VERA-51333	45.493	-1.144	Amélie beach, Soulac
	This study	¹⁴ C	1330 ±50	1345 (1259) 1152	605 (691) 798	Amelie beach	Palaeosol 1 (section 3)	VERA-51334	45.497	-1.142	Amélie beach, Soulac
	This study	¹⁴ C	1720 ±125	1897 (1639) 1356	53 (311) 594	Amelie beach	Palaeosol 0 (section dune toe)	VERA-51401	45.496	-1.142	Amélie beach, Soulac
	This study	¹⁴ C	1733 ±46	1780 (1647) 1539	170 (303) 411	Amelie beach	Palaeosol 0 (section 28)	VERA-51398	45.488	-1.148	Amélie beach, Soulac
	This study	¹⁴ C	1920 ±70	2039 (1864) 1638	-89 (86) 312	Amelie beach	Palaeosol 0 (section 21)	VERA-51339	45.492	-1.146	Amélie beach, Soulac
	This study	¹⁴ C	2025 ±60	2145 (1985) 1865	-195 (-35) 85	Amelie beach	Palaeosol 0 (section 25)	VERA-51337	45.490	-1.147	Amélie beach, Soulac
Le Pyla dune											
stability phases	Tastet (1998)	¹⁴ C	320 ±60	502 (388) 157	1448 (1562) 1793	TM 96016	wood in palaeosol 3	Beta 95381	44.59	-1.21	Le Pyla dune
	Froidefond & Legigan (1985)	¹⁴ C	2690 ±70	2966 (2813) 2715	-1016 (-863) -765		Charcoal in the sand above palaeosol 2	LRGMR Bx	44.59	-1.21	Le Pyla dune
	Froidefond & Legigan (1985)	¹⁴ C	2980 ±110	3332 (3148) 2862	-1382 (-1198) -912		wood in palaeosol 2	Gif	44.59	-1.21	Le Pyla dune
	Tastet (1998)	¹⁴ C	3080 ±60	3445 (3285) 3082	-1495 (-1335) -1132	TM 96013	wood in palaeosol 2	Beta 95378	44.59	-1.21	Le Pyla dune
	Tastet (1998)	¹⁴ C	3180 ±60	3561 (3406) 3249	-1611 (-1456) -1299	TM 96012	wood in palaeosol 2	Beta 95377	44.59	-1.21	Le Pyla dune
	Tastet (1998)	¹⁴ C	3220 ±70	3612 (3449) 3255	-1662 (-1499) -1305	TM 96015	sandy peat in the base of palaeosol 1	Beta 95380	44.59	-1.21	Le Pyla dune
	Tastet (1998)	¹⁴ C	3310 ±70	3696 (3542) 3387	-1746 (-1592) -1437	TM 96014	peat at the top of palaeosol 1	Beta 95379	44.59	-1.21	Le Pyla dune
	Froidefond & Legigan (1985)	¹⁴ C	3460 ±70	3905 (3731) 3563	-1955 (-1781) -1613		wood in palaeosol 1	Gif	44.59	-1.21	Le Pyla dune
	Tastet (1998)	¹⁴ C	3490 ±60	3912 (3765) 3608	-1962 (-1815) -1658	TM 97001	wood in palaeosol 1	Beta 102698	44.59	-1.21	Le Pyla dune
	Tastet (1998)	¹⁴ C	3510 ±70	3973 (3785) 3615	-2023 (-1835) -1665	TM 96023	wood in palaeosol 1	Beta 95382	44.59	-1.21	Le Pyla dune
	Froidefond & Legigan (1985)	¹⁴ C	3680 ±110	4401 (4025) 3714	-2451 (-2075) -1764		wood in palaeosol 1	LRGMR Bx	44.59	-1.21	Le Pyla dune
activity phases	Clarke et al. (1999)	IRSL	305 ±25	268 (255) 243	1683 (1695) 1708		aeolian sand	PA7	44.59	-1.21	Le Pyla dune
	Clarke et al. (1999)	IRSL	935 ±120	990 (885) 780	960 (1065) 1170		aeolian sand	PA5	44.59	-1.21	Le Pyla dune
	Clarke et al. (1999)	IRSL	3350 ±310	3610 (3300) 2990	-1660 (-1350) -1040		aeolian sand	PA4	44.59	-1.21	Le Pyla dune
	Clarke et al. (1999)	IRSL	3645 ±460	4055 (3595) 3135	-2105 (-1645) -1185		aeolian sand	PA3	44.59	-1.21	Le Pyla dune
	Clarke et al. (1999)	IRSL	3520 ±315	3785 (3470) 3155	-1835 (-1520) -1205		aeolian sand	PA1	44.59	-1.21	Le Pyla dune

Tab. 5: Chronological data available on the Holocene evolution of the Aquitaine coastal dunes.

Tab. 5 : Données chronologiques disponibles sur l'évolution holocène des dunes côtières d'Aquitaine.

with data available for the Aquitaine region (Dubreuilh, 1971; Froidefond & Legigan, 1985; Tastet, 1998; Clarke *et al.*, 1999, 2002). While the data on the Médoc dune system and Le Pilat dune reveal numerous common phases of dune stability and aeolian activity, the long-term morphological changes of the L'Amélie dunes present a specific chronology. Along L'Amélie beach, this chronology is limited to the last 2000 years, while the peat layers studied along the Médoc coastal dunes cover a long time period indicating two previous phases of dune fixation, dated at ca. 6000 cal. a BP (Dubreuilh, 1971) and from ca. 4000 to ca. 3000 cal. a BP (Dubreuilh, 1971 ; Tastet & Pontee, 1998). During the last 2000 years, the only common phase of dune stability with the Médoc dune system is represented by palaeosol 0 dated from 1990 to 1650 cal. a BP (median calibrated ages). No synchronicity is observed in the formation of palaeosols between L'Amélie beach and the Dune du Pilat, except for the humic layer observed in the L'Amélie dune sequence that may correspond to palaeosol 3 of the Dune du Pilat dated to 320-157 cal. a BP (Tastet, 1998).

Several authors attempted to explain the long-term morphological evolution of coastal dunes of Aquitaine depending on factors such as (i) sediment supply related to coastal erosion by severe storms, (ii) positive or negative variation of RSL during the last 6000 cal. a BP, (iii) changes in vegetation cover, and (iv) increased windiness and storminess. Previous work has favoured dune formation under falling RSL and cooler climatic conditions which, through coastal exposure, supplied sand to the dunes whilst positive RSL tendencies favoured the erosion of the coast and the fixation of the dunes by a more humid climate and a rise in groundwater levels. The evolution of the Médoc peninsula was interpreted as being formed under a series of positive and negative RSL tendencies that affected the area after 6000 cal. a BP (Pontee *et al.*, 1998). However, the RSL records produced in this paper are not reliable enough to confirm periods of significant fall in RSL over the last millennia. In the Dune du Pyla area, Bressolier *et al.* (1990) also believed that dunes were active during regressive periods, but also considered climatic change to be important. On the dune barrier lining the southern North Sea, Anthony *et al.* (2010) recently highlighted the role played by repeated storms into the mid-Holocene dune formation. The onshore transfer of tidal-bank sand generates pulses of abundant sand supply and an extremely rapid progradation (up to 1 km over a century) of the sand-flat shore, the surface of which serves as a large aeolian fetch zone for active backshore dune accumulation. Because of the vicinity of the Gironde mouth, the long-term morphological changes of L'Amélie beach/dune system are very sensitive to variations in sediment supplies provided by the estuary through the onshore migration of tidal sandbanks. On a short time scale (decadal), Castelle *et al.* (2018) highlighted the high spatio-temporal variability of the shoreline at the mouths along the coasts of Charentes and Aquitaine through a very active coastal erosion process over the last decades. Historical records from Roman times, bathymetric

maps dating back to the seventeenth century and recent bathymetric surveys also indicate great morphological changes of the sandbanks along the Gironde mouth over the last centuries (Allen *et al.*, 1974; Kapsimalis *et al.*, 2004). Analysis of these bathymetric data indicates the initial construction of sandbanks and high volumes of sediment transfer leading to their migration over the past three centuries. Effects on the long-term evolution of the North Médoc dune system are very difficult to estimate because of the very dynamic nature of these coastal features and the numerous feedbacks between hydrodynamic and morphosedimentary factors (e.g. the modulation of incident storm-wave energy variations alongshore depending on the location and the morphology of sandbanks). Nevertheless, the variability of shoreface sand supply related to wave and wind climate changes seems to provide a template for a better understanding of the late Holocene coastal dune evolution of the storm-dominated Médoc peninsula.

6 - CONCLUSIONS

The recent 2013-2014 erosion events exposed mid- to late-Holocene sedimentary records along L'Amélie beach (locality of Soulac, SW France) that have been intensively studied using topographical surveys and sedimentological analyses of deposits cropping out in the intertidal zone. This paper presents the resulting comprehensive chronostratigraphic and palaeoenvironmental framework that greatly increases our understanding not only of the long-term coastal evolution of this specific part of France, but also -by comparing the established evolution with supra-regional palaeoenvironmental changes- of the variation in driving factors like sea-level change, sediment availability and the wind regime.

From bottom to top, the Holocene sequence exhibits 10 main lithofacies:

- Unit 1 corresponds with Pleistocene deposits represented by a 2 m-thick compact dark-green clay dated to MIS 9, overlain by a gravelly sandstone dated to MIS 2;

- Unit 2 is composed of a very well sorted medium to coarse sand deposit, dated to ca. 7290 cal. a BP and interpreted as the gradual infilling of a large tidal channel;

- Unit 3 consists of a set of organic to minerogenic silty clay deposits with a sharp erosion surface characterized by the presence of reworked gravelly lithoclasts of humate-impregnated sandstone, locally associated with a pavement of *Scrobicularia* shells dated to 3434-3070 cal. a BP. These deposits suggest the development of estuarine salt marshes and mud-flats, then their erosion by waves;

- Units 4 and 5 are formed by a clayey-silt deposit with foraminiferal assemblages dominated by intertidal mudflat species, and by an organic-rich clayey-silt with foraminiferal content indicating a salt marsh environment, respectively. Radiocarbon datings and abundant archaeological evidence indicate the presence

of a back-barrier environment along the present-day coastline of L'Amélie beach from ca. 2700 to ca. 1000 cal. a BP;

- Units 6 to 10 are a succession of aeolian sand deposits separated by three layers of palaeosols or organic-rich sediments dated to ca. 1990 cal. a BP to the present-day.

The sedimentary sequences are indicative of:

- a significant Holocene sedimentary sequence composed of coastal material deposited in a large depression located in the central part of L'Amélie beach;

- the presence of a large tidal channel filled by coarse sand during the first stage of the Holocene sea-level upstand from ca. 7000 to ca. 5000 cal. a BP;

- fine-grained estuarine sedimentation behind a coastal dune barrier from ca. 5000 to 2700 a cal. BP, interrupted by an episode of coastal erosion between 3500 and 3000 cal. a BP;

- gradual burial of the estuarine salt marshes with aeolian sands from ca. 1900 to 1200 cal. a BP;

- two main periods of coastal dune stability dated from 1990 to 1640 cal. a BP (palaeosol 0) and from 1260 to 1010 cal. a BP, respectively.

Despite the usefulness of these initial results for better interpreting the coastal archaeological contexts of the North Médoc, further research is still required to (i) better constrain the history of palaeogeographic changes over the last ca. 7000 years, (ii) achieve a better understanding of the aeolian activity based on the absolute dating of the aeolian sand material, and (iii) estimate the influence of these coastal changes on human settlement strategies over time.

The reconstructed sequence of palaeogeographic changes highlights the high mobility of this part of the French Atlantic coastline during the last millennia. At the present-time, the dune barrier of the North Médoc is experiencing significant erosion. The shoreline retreat threatens many urbanized areas and requires consideration of appropriate spatial planning strategies. This context makes it essential to develop integrated approaches combining the monitoring of short-term coastal dynamics and a better knowledge of long-term changes in order to better understand the morphosedimentary processes at work and predict future changes of the coastline.

ACKNOWLEDGMENTS

This study has been carried out with financial support from the French National Research Agency (ANR) in the framework of the Investments for the future Programme, within the Cluster of Excellence COTE (ANR-10-LABX-45) and within the Cluster of Excellence LaScArBx (ANR-10-LABX-45). Romain Cancouët and Ronan Autret are thanked for their valuable help in the field. The authors are very grateful to Eric Chaumillon and Marc P. Hijma for their constructive comments.

REFERENCES

- ANTHONY E.J., MRANI-ALAOUI M. & HÉQUETTE A., 2010 - Shoreface sand supply and mid- to late Holocene aeolian dune formation on the storm-dominated macrotidal coast of the southern North Sea. *Marine Geology*, **276**, 100-104.
- ALLARD A., DUBREUILH J. & MARIONNAUD J.M., 1974 - Contribution à la résolution d'un problème de géologie récente : exemple du Bas-Médoc (Gironde). *Bulletin du BRGM*, **2** (1), 1-14.
- ALLARD J., CHAUMILLON E. & FÉNIÈS H., 2009 - A synthesis of morphological evolutions and Holocene stratigraphy of a wave-dominated estuary: The Arcachon lagoon, SW France. *Continental Shelf Research*, **29**, 957-969.
- ALLEN G.P., BOUCHET J.-M., CARBONEL P., CASTAING P., GAYET J., GONTIER E., JOUANNEAU J.-M., KLINGEBIEL A., LATOUCHE C., LEGIGAN P., ORGERON C., PUJOS M., TESSON M. & VERNETTE G., 1974 - Environnements et processus sédimentaires sur le littoral nord-Aquitain. *Bulletin de l'Institut de Géologie du Bassin d'Aquitaine*, **15**, 3-183.
- ALLEN G.P., CASTAING P. & TASTET J.-P., 1981 - Excursion géologique sur l'estuaire de la Gironde, 19-20 mai 1981. Compagnie Française des Pétroles & de l'Institut de Géologie du Bassin d'Aquitaine, Bordeaux, 121 p.
- ALLEN G.P., 1991 - Sedimentary processes and facies in the Gironde Estuary: a recent model for macrotidal estuarine systems. *Canadian Society of Petroleum Geologists*, **16**, 29-40.
- ALLEN G.P. & POSAMENTIER H.W., 1993 - Sequence Stratigraphy and Facies Model of an Incised Valley Fill: The Gironde Estuary, France. *Journal of Sedimentary Petrology*, **63** (3), 378-391.
- ALLEN J.R.L., 2000 - Holocene coastal lowlands in NW Europe: autocompaction and the uncertain ground. In K. Pye & J.R.L. Allen (eds.), *Coastal and Estuarine Environments: sedimentology, geomorphology and gearchaeology*, Geological Society, Special Publication, London, **175**, 239-252.
- ALLEN J.R.L., 2003 - An eclectic morphostratigraphic model for the sedimentary response to Holocene sea-level rise in northwest Europe. *Sedimentary Geology*, **161**, 31-54.
- ANDERSON J.B., RODRIGUEZ A.B., MILLIKEN K. & TAVIANI M., 2008 - The Holocene evolution of the Galveston estuary complex, Texas: Evidence for rapid change in estuarine environments. *The Geological Society of America, Special Paper*, **443**, 89-104.
- ARMYNOT DU CHATELET E., DEBENAY J.-P., DEGRE D. & SAURIAU P.-G., 2005 - Utilisation des foraminifères benthiques comme indicateurs de paléo-niveaux marins? Etude du cas de l'anse de l'Aiguillon. *Comptes Rendus Palévol*, **4**, 209-223.
- ASHE E.L., CAHILL N., HAY C.C., KHAN N.S., KEMP A.C., ENGELHART S.E., HORTON B.P., PARNELL A.C. & KOPP R.E., 2019 - Statistical modeling of rates and trends in sea level. *Quaternary Science Reviews*, **204**, 58-77.
- AUBIE S. & TASTET J.-P., 2000 - Coastal erosion, processes and rates: an historical study of the Gironde Coastline, Southwestern France. *Journal of Coastal Research*, **16**, 756-767.
- BARBER K.E., CHAMBERS F.M. & MADDY D., 2003 - Holocene palaeoclimates from peat stratigraphy: macrofossil proxy climate records from three oceanic raised bogs in England and Ireland. *Quaternary Science Reviews*, **22**, 521-539.
- BARBER K.E., CHAMBERS F.M. & MADDY D., 2004 - Late Holocene climatic history of northern Germany and Denmark: peat macrofossil investigations at Dosenmoor, Schleswig-Holstein, and Svanemose, Jutland. *Boreas*, **33**, 132-144.
- BAUMANN J., CHAUMILLON E., BERTIN X., SCHNEIDER J.-L., GUILLOT B. & SCHMUTZ M., 2017 - Importance of infragravity waves for the generation of washover deposits. *Marine Geology*, **391**, 20-35.
- BEAUVIAL C., MICHEL P. & TASTET J.-P., 1998 - L'éléphant antique de Soulac (Gironde, France). *Quaternaire*, **9**, 91-100.
- BERTIN X., CASTELLE B., CHAUMILLON E., BUTEL R. & QUIQUE R., 2008 - Longshore transport estimation and inter-annual variability at a high-energy dissipative beach: St. Trojan beach, SW Oléron Island, France. *Continental Shelf Research*, **28**, 10-11, 1316-1332.
- BILLEAUD I., TESSIER B. & LESUEUR P., 2009 - Impacts of Late Holocene rapid climate changes as recorded in a macrotidal coastal setting (Mont-Saint-Michel Bay, France). *Geology*, **37**, 1031-1034.
- BOSQ M., BERTRAN P., BEAUVIAL C., KREUTZER S., DUVAL M., BARTZ M., MERCIER N., SITZIA L. & STÉPHAN P., 2019 - Stratigraphy and chronology of Pleistocene coastal deposits in Northern Aquitaine, France: a reinvestigation. *Quaternaire*, **30**, 5-20.

- BOURGUEIL B., 1995** - Datations au radiocarbone de niveaux tourbeux holocènes du marais de Rochefort (Charente-Maritime) : Variation du niveau marin au cours du 9e millénaire (BP). *Géologie de la France*, **1995-1**, 77-80.
- BOURGUEIL B., 2005** - Evolution de la transgression flandrienne et du littoral charentais depuis 8500 BP. *Géologie de la France*, **2005-1**, 75-84.
- BOYD R., DALRYMPLE R.W. & ZAITLIN B.A., 2006** - Estuarine and incised-valley facies models. In H. Posamentier & R. Walker (eds.), *Facies Models Revisited*. SEPM Special Publication **84**. Society for Sedimentary Geology, Tulsa, 171-235.
- BRESSOLIER C., FROIDEFOND J.M. & THOMAS Y.F., 1990** - Chronology of coastal dunes in the Southwest of France. *Catena Supplement*, **18**, 101-107.
- BROOKFIELD M.E. & AHLBRANDT T.S., 1983** - *Eolian Sediments and Processes*. Elsevier, Amsterdam, **38**, 659 p.
- BRUNEAU N., BONNETON P., CASTELLE B. & PEDREROS R., 2011** - Modeling rip current circulations and vorticity in a high-energy meso-macrotidal environment. *Journal of Geophysical Research*, **116**, C07026.
- BUFFAULT P., 1942** - *Histoire des dunes maritimes de Gascogne*. Bordeaux, Imprimerie Delmas, 446 p.
- BULTEAU T., MUGICA J., MALLET C., GARNIER C., ROSE-BERY D., MAUGARD F., NICOLAE LERMA A. & NAHON A., 2014** - Évaluation de l'impact des tempêtes de l'hiver 2013-2014 sur la morphologie de la Côte Aquitaine. Rapport final BRGM/RP-63797-FR, Novembre 2014, 184 p.
- BUTTEL R., DUPUIS H. & BONNETON P., 2002** - Spatial variability of wave conditions on the French Atlantic coast using in situ data. *Journal of Coastal Research. Special Issue*, **36**, 96-108.
- CARBONEL P., 1980** - *Les Ostracodes et leur intérêt dans la définition des écosystèmes estuariens et de la plateforme continentale. Essais d'application à des domaines anciens*. Mémoires IGBA, **11**, 1-350.
- CASTELLE B., MARIEU V., BUJAN S., FERREIRA S., PARISOT J.P., CAPO S., SENECHAL N. & CHOUZENOUX T., 2014** - Equilibrium shoreline modelling of a high-energy meso-macrotidal multiple-barred beach. *Marine Geology*, **347**, 85-94.
- CASTELLE B., MARIEU V., BUJAN S., SPLINTER K.D., ROBINET A., SÉNÉCHAL N. & FERREIRA S., 2015** - Impact of the winter 2013-2014 series of severe Western Europe storms on a double-barred sandy coast: Beach and dune erosion and megacusps embayments. *Geomorphology*, **238**, 135-14.
- CASTELLE B., GUILLOT B., MARIEU V., CHAUMILLON E., HANQUIEZ V., BUJAN S. & POPPESCHI C., 2018** - Spatial and temporal patterns of shoreline change of a 280-km high-energy disrupted sandy coast from 1950 to 2014: SW France. *Estuarine, Coastal and Shelf Science*, **200**, 212-223.
- CHARMAN D.J., 2010** - Centennial climate variability in the British Isles during the mid-late Holocene. *Quaternary Science Reviews*, **29**, 1539-1554.
- CHAUMILLON E., TESSIER B. & REYNAUD J.-Y., 2010** - Stratigraphic records and variability of incised valleys and estuaries along the French coasts. *Bulletin de la Société Géologique de France*, **181**, 2, 75-85.
- CHAUMILLON E., FÉNIÈS H., BILLY J., BREILH J.-F. & RICCHETTI H., 2013** - Tidal and fluvial controls on the internal architecture and sedimentary facies of a lobate estuarine tidal bar (The Plassac Tidal Bar in the Gironde Estuary, France). *Marine Geology*, **346**, 58-72.
- CLARKE M.L. & RENDELL H.M., 2009** - The impact of North Atlantic storminess on western European coasts: A review. *Quaternary International*, **195**, 31-41.
- CLARKE M., RENDELL H., PYE K., TASTET J.P., PONTEE N.I. & MASSÉ L., 1999** - Evidence for the timing of dune of dune development on the Aquitaine coast, southwest France. *Zeitschrift für Geomorphologie N.F. Supplement Band*, **116**, 147-63.
- CLARKE M., RENDELL H., TASTET J.-P., CLAVÉ B. & MASSÉ L., 2002** - Late-Holocene sand invasion and North Atlantic storminess along the Aquitaine Coast, southwest France. *The Holocene*, **12** (2), 231-238.
- CLAVÉ B., MASSÉ L., CARBONEL P. & TASTET J.-P., 2001** - Holocene coastal changes and infilling of the La Perroche marsh (French Atlantic coast). *Oceanologica Acta*, **24**, 377-389.
- CLAVÉ B., 2001** - *Evolution des paléo-environnements côtiers à l'Holocène : exemple de l'Aquitaine septentrionale*. Thèse de doctorat, Université Bordeaux 1, Bordeaux, 316 p.
- CLEMENT A.J.H., FULLER I.C. & SLOSS C.R., 2017** - Facies architecture, morphostratigraphy, and sedimentary evolution of a rapidly-infilled Holocene incised-valley estuary: The lower Manawatu valley, North Island New Zealand. *Marine Geology*, **390**, 214-233.
- COSTAS S., JEREZ S., TRIGO R.M., GOBLE R. & REBÊLO L., 2012** - Sand invasion along the Portuguese coast forced by westerly shifts during cold climate events. *Quaternary Science Reviews*, **42**, 15-28.
- CRESSIE N. & WIKLE C.K., 2011** - *Statistics for spatio-temporal data*. John Wiley & Sons, 588 p.
- DALRYMPLE R.W., ZAITLIN B.A. & BOYD R., 1992** - Estuarine Facies Models: Conceptual Basis and Stratigraphic Implications: perspective. *Journal of Sedimentary Petrology*, **62** (6), 1130-1146.
- DANIELSEN R., CASTILHO A.M., DINIS P.A., ALMEIDA A.C. & CALLAPEZ P.M., 2012** - Holocene interplay between a dune field and coastal lakes in the Quiaios-Tocha region, central littoral Portugal. *The Holocene*, **22**, 383-395.
- DARK P., 2006** - Climate deterioration and land-use change in the first millennium BC: perspectives from the British palynological record. *Journal of Archaeological Science*, **33**, 1381-1395.
- DEBENAY J.-P., BICCHI E., GOUBERT E. & ARMYNOT DU CHÂTELET E., 2006** - Spatio-temporal distribution of benthic foraminifera in relation to estuarine dynamics (Vie estuary, Vendée, W France). *Estuarine, Coastal and Shelf Science*, **67**, 181-197.
- DELAINÉ M., ARMYNOT DU CHÂTELET E., BOUT-ROUMAZIELLES V., GOUBERTE, LE CADRE V., RECOURT P., TRENTESAUX A. & ARTHUIS R., 2015** - Multi-proxy approach for Holocene paleoenvironmental reconstructions from microorganisms (testate amoebae and foraminifera) and sediment analyses: The infilling of the Loire Valley in Nantes (France). *The Holocene*, **25** (3), 407-420.
- DIOT M.-F. & TASTET J.-P., 1995** - Paléo-environnements holocènes et limites chrono-climatiques enregistrés dans un marais estuaire de la Gironde (France). *Quaternaire*, **6** (2), 63-75.
- DIOT M.-F., MARAMBAT L., MASSE L. & TASTET J.-P., 2001** - Etude palynologique du remplissage holocène du marais de Reysson, rive gauche de la Gironde, Nord-Médoc (France). Relation avec l'occupation humaine. In J. L'Helgouach & J. Briard (dirs.), *Systèmes fluviaux, estuaires et implantations humaines : de la préhistoire aux grandes invasions*. Editions du CTHS, Paris 143-162.
- DUBREUILH J., 1971** - *Etude géologique des formations quaternaires du Bas-Médoc. Essai de corrélations stratigraphiques*. Thèse de doctorat, Université Bordeaux 1, Bordeaux ; 158 p.
- DUCHEMIN G., JORISSEN F.J., REDOIS F. & DEBENAY J.-P., 2005** - Foraminiferal microhabitats in a high marsh: consequences for reconstructing past sea levels. *Palaeogeography, Palaeoclimatology, Palaeoecology*, **226**, 167-185.
- DURAND M., MOJTAHID M., MAILLET G.M., PROUST J.-N. & HOWA H., 2016** - Mid- to late-Holocene environmental evolution of the Loire estuary as observed from sedimentary characteristics and benthic foraminiferal assemblages. *Journal of Sea Research*, **118**, 17-34.
- FAVENNEC J., GRANJA H., PRAT M.-C., HALLEGOUËT B., YONI Y., BARRERE P., ROZE F., JUN R., DAUPHIN P., THOMAS H., ESTEVE G., MICHENEAU C., THIRION J.-M., VENEAU F., LAHONDERE C., LEBON P., SALOMON J.-N., OYARZABAL J., GRANEREAU G., JARRET J., RICHARD P., DIENG D., DUFFAUD M.-H., FEVRIER G., METAYER S. & GOUGUET L., 2002** - *Connaissance et gestion durable des dunes de la côte atlantique. Manuel récapitulant les enseignements du projet européen LIFE-Environnement de « Réhabilitation et gestion durable de quatre dunes françaises »*. Coll. « LES DOSSIERS FORESTIERS », n°11, Ed. Office National des Forêts, Paris, 380 p.
- FÉNIÈS H. & TASTET J.-P., 1998** - Facies and architecture of an estuarine tidal bar (the Trompeloup Bar, Gironde Estuary, SW France). *Marine Geology*, **150**, 149-169.
- FÉNIÈS H. & LERICOLAIS G., 2005** - Internal architecture of an incised valley-fill on a wave- and tide- dominated coast (the Leyre incised valley, Bay of Biscay, France). *Comptes Rendus Geosciences*, **337** (14), 1257-1266.
- FÉNIÈS H., LERICOLAIS G. & POSAMENTIER H.W., 2010** - Comparison of wave-and tide-dominated incised valleys: specific processes controlling systems tract architecture and reservoir geometry. *Bulletin de la Société géologique de France*, **181** (2), 171-181.
- FLETCHER C.H., KNEBEL H.J. & KRAFT J.C., 1990** - Holocene evolution of an estuarine coast and tidal wetlands. *Geological Society of America Bulletin*, **102**, 283-297.
- FOLK R.L. & WARD W.C., 1957** - A Study in the Significance of Grain-Size Parameters. *Journal of Sedimentary Petrology*, **27**, 3-26.
- FROIDEFOND J.M. & LEGIGAN P., 1985** - La grande dune du Pilat et la progression des dunes sur le littoral aquitain. *Bulletin de l'Institut de Géologie du Bassin d'Aquitaine*, **38**, 69-79.

- FROIDEFOND J.M., 1982** - *Processus d'évolution d'un littoral sableux au cours de l'Holocène. Application au domaine aquitain. Présentation d'une méthode de géomorphologie dynamique et quantitative.* Thèse de Doctorat d'Etat n°724, Université Bordeaux 1, Bordeaux, 273 p.
- GABET C., 1973** - Le banc de tourbe sur l'estran de la baie de Perroche (Île d'Oléron). *Recueil de la Société d'Archéologie et d'Histoire de la Charente Maritime*, **25**, 297-307.
- GANDOUIN E., PONEL P., ANDRIEU-PONEL V., GUITER F., DE BEAULIEU J.L., DJAMALI M., FRANQUET E., VAN VLIET-LANOË B., ALVITRE M., MEURISSE M., BROCANDEL M. & BRULHET J., 2009** - 10,000 years of vegetation history of the Aa palaeoestuary, St-Omer Basin, northern France. *Review of Palaeobotany and Palynology*, **156**, 307-318.
- GARCÍA-ARTOLAA A., STÉPHAN P., CEARRETA A., KOPP R.E., KHAN N.S. & HORTON B.P., 2018** - Holocene sea-level database from the Atlantic coast of Europe. *Quaternary Science Reviews*, **196**, 177-192.
- GOURDON-PLATEL A. & MORIN B., 2004** - Le fer des marais, encroûtement superficiel holocène utilisé sur les sites archéologiques de Sanguinet (Landes, France). *Géologie de la France*, **1**, 13-24.
- GOUBERT E., 1997** - *Les Elphidium excavatum (Terquem), foraminifères benthiques, vivants en baie de Vilaine (Bretagne, France) d'octobre 1992 à septembre 1996 : morphologie, dynamique de population en relation avec l'environnement.* Thèse de doctorat, Université de Nantes, Nantes, 186 p.
- HESP P., 1988** - Morphology, dynamics and internal stratification of some established foredunes in southeast Australia. *Sedimentary Geology*, **55**, 17-41.
- HIJMA M.P., ENGELHART S.E., TÖRNQVIST T.E., HORTON B.P., HU P. & HILL D.F., 2015** - A protocol for a geological sea-level database. In I. Shennan, A.J. Long & B.P. Horton (eds.) *Handbook of Sea-Level Research*, John Wiley & Sons, Ltd., 536-554.
- IDIER D., CASTELLE B., CHARLES E. & MALLET C., 2013** - Longshore sediment flux hindcast: spatiotemporal variability along the SW Atlantic coast of France. *Journal of Coastal Research, Special Issue*, **65**, 1785-1790.
- KAPSIMALIS V., MASSÉ L., VELEGRAKIS A., TASTET J.P., LAGASQUIE M.H. & PAIREAU O., 2004** - Formation and growth of an estuarine sandbank: Saint-Georges Bank, Gironde Estuary(France). *Journal of Coastal Research*, **41**, 27-42.
- KOCIUBA W., KUBISZ W. & ZAGÓRSKI P., 2014** - Use of terrestrial laser scanning (TLS) for monitoring and modelling of geomorphic processes and phenomena at a small and medium spatial scale in Polar environment (Scott River-Spitsbergen). *Geomorphology*, **212**, 84-96.
- KOPP R.E., KEMP A.C., BITTERMANN K., HORTON B.P., DONNELLY J.P., GEHRELS W.R., HAY C.C., MITROVICA J.X., MORROW E.D. & RAHMSTORF S., 2016** - Temperature-driven global sea-level variability in the Common Era. *Proceedings of the National Academy of Sciences of the USA*, **113**, E1434-1441.
- LAMB H.H. & FRYDENDAHL K., 2005** - *Historic Storms of the North Sea, British Isles and Northwest Europe.* Cambridge University Press, Cambridge, 228 p.
- LAMBECK K., 1997** - Sea-level change along the French Atlantic and Channel coast since the time of the Last Glacial Maximum. *Palaeogeography, Palaeoclimatology, Palaeoecology*, **129**, 1-22.
- LAPEN D.R. & WANG C., 1999** - Placic and ortstein horizon genesis and peatland development, southwestern Newfoundland. *Soil Science Society of America Journal*, **63**, 1472-1482.
- L.C.H.F. 1979** - *Etude en nature de la côte aquitaine.* Rapport général pour la D.A.T.A.R., M.I.A.C.A., Maisons Alfort, 4 tomes.
- L.C.H.F. 1982** - *Etude de l'évolution du littoral de la côte aquitaine entre la Pointe de Grave et l'embouchure de l'Adour.* Rapport de mission L.C.H.F.-M.I.A.C.A., Maisons Alfort, 52 p.
- L.C.H.F. 1987** - *Catalogue sédimentologique des côtes françaises : côtes de la Manche et de l'Atlantique de la baie du Mont Saint-Michel à la frontière espagnole, Partie C: de la Gironde à la frontière espagnole.* Collection Direction Etudes Recherches E.D.F., Ed. Eyrolles, **65**, 371-552.
- LEORRI E., GEHRELS W.R., HORTON B.P., FATELA F. & CEARRETA A., 2010** - Distribution of foraminifera in salt marshes along the Atlantic coast of SW Europe: Tools to reconstruct past sea-level variations. *Quaternary International*, **221**, 104-115.
- LERICOLAIS G., FENIES H., TASTET J.-P. & BERNE S., 1998** - Reconnaissance par stratigraphie sismique haute résolution de la paléovallée de la Gironde sur le plateau continental. *Comptes Rendus de l'Académie des Sciences. Série 2. Sciences de la Terre et des Planètes*, **326**, 701-708.
- LESPEZ L., CLET-PELLERIN M., DAVIDSON R., HERMIER G., CARPENTIER V. & CADOR J.-M., 2010** - Middle to Late Holocene landscape changes and geoarchaeological implications in the marshes of the Dives estuary (NW France). *Quaternary International*, **216**, 23-40.
- LESUEUR P. & TASTET J.-P., 1994** - Facies, internal structures and sequences of modern Gironde-derived muds on the Aquitaine inner shelf, France. *Marine Geology*, **120**, 267-290.
- LICHTI D.D., GORDON S.J. & STEWART M.P., 2002** - Ground-based laser scanners: operation, systems and applications. *Geomatica*, **56**, 22-33.
- LONG A.J. & HUGHES P.D.M., 1995** - Mid- and late-Holocene evolution of the Dungeness foreland, UK. *Marine Geology*, **124**, 253-271.
- MAGNY M., 2004** - Holocene climate variability as reflected by mid-European lake-level fluctuations and its probable impact on prehistoric human settlements. *Quaternary International*, **113**, 65-79.
- MARAMBAT L., 1992** - *Paléoenvironnements et empreinte anthropique dans l'ouest aquitain et la saintonge à l'Holocène. L'apport de la palynologie.* Thèse de doctorat, Université Bordeaux I, Bordeaux, 269 p.
- MARIONNAUD J.M. & DUBREUILH J., 1972** - *Carte géologique de France (1/50000), feuille St Vivien - Soulac (729-730).* Editions BRGM, Orléans, 41 p.
- MICHEL D. & HOWA H., 1999** - Short-term morphodynamic response of a ridge and runnel system on a mesotidal sandy beach. *Journal of Coastal Research*, **15**, 428-437.
- MOULINIER M., 1966** - Variabilité d'une population d'Elphidium de la rade de Brest (Nord Finistère) apparentées à *Elphidium crispum* (Linné). *Revue de Micropaléontologie*, **9**, 124-200.
- MOURA D., VEIGA-PIRES L., ALBARDEIRO T., BOSKI T., RODRIGUES A.L. & TARECO H., 2007** - Holocene sea level fluctuations and coastal evolution in the central Algarve (southern Portugal). *Marine Geology*, **237**, 127-142.
- MURRAY J.W., 1979** - British Nearshore Foraminiferids. Synopses of the British Fauna (New Series), **16**. Academic Press, London, New York & San Francisco, 66 p.
- OERTLI H.J., 1985** - *Atlas des ostracodes de France.* Bulletin du Centre de Recherche, Exploration et Production Elf-Aquitaine, Mémoire n°9, 53 p.
- PACKHAM J.R. & WILLIS A.J., 1997** - *Ecology of Dunes, Salt Marsh and Shingle,* Ed. Springer US, 335 p.
- PONTEE N.I., TASTET J.-P. & MASSÉ L., 1998** - Morphosedimentary evidence of Holocene coastal changes near the mouth of the Gironde and on the Medoc Peninsula, SW France. *Oceanologica Acta*, **21** (2), 243-261.
- PYE K. & TSOAR H., 2009** - *Aeolian Sand and Sand Dunes.* Springer, Berlin & Heidelberg, 458 p.
- REDOIS F. & DEBENAY J.-P., 1996** - Influence du confinement sur la répartition des foraminifères benthiques: exemple de l'estran d'une ria mésotidale de Bretagne méridionale. *Revue de Paléobiologie*, **15**, 243-260.
- REIMER P.J., BARD E., BAYLISS A., BECK J.W., BLACKWELL P.J., RAMSEY C.B., BUCK C.E., CHENG H., EDWARDS R.L., FRIEDRICH M., GROOTES P.M., GUILDERSON T.P., HAFLIDASON H., HAJDAS I., HATTE C., HEATON T.J., HOFFMANN D.L., HOGG A.G., HUGHEN K.A., KAISER K.F., KROMER B., MANNING S.W., NIU M., REIMER R.W., RICHARDS D.A., SCOTT E.M., SOUTHON J.R., STAFF R.A., TURNER C.S.M. & VAN DER PLICHT J., 2013** - Intcal13 and Marine13 radiocarbon age calibration curves 0-50,000 years cal BP. *Radiocarbon*, **55**, 1869-1887.
- REINECK H.E. & SINGH I.B., 1980** - *Depositional Sedimentary Environments.* Springer, Berlin, 549 p.
- ROSSI V., HORTON B.P., CORBETT D.R., LEORRI E., PEREZ-BELMONTE L. & DOUGLAS B.C., 2011** - The application of foraminifera to reconstruct the rate of 20th century sea level rise, Morbihan Golfe, Brittany, France. *Quaternary Research*, **75**, 24-35.
- RUIZ F., GONZALEZ-REGALADO M.L., BACETA J.I. & MUÑOZ J.M., 2000** - Comparative ecological analysis of the ostracod faunas from low- and high-polluted southwestern Spanish estuaries: a multivariate approach. *Marine Micropaleontology*, **40**, 345-376.
- RUIZ F., RODRÍGUEZ-RAMÍREZ A., CÁCERES L.M., VIDAL J.R., CARRETERO M.I., CLEMENTE L., MUÑOZ J.M., YAÑEZ C. & ABAD M., 2004** - Late Holocene evolution of the southwestern Donana National Park (Guadalquivir Estuary, SW Spain): a multivariate approach. *Palaeogeography, Palaeoclimatology, Palaeoecology*, **204**, 47-64.

- SCHNEIDER H., HÖFER D., TROG C., BUSCH S., SCHNEIDER M., BAADE J., DAUT G. & MÄUSBACHER R., 2010** - Holocene estuary development in the Algarve Region (Southern Portugal)- A reconstruction of sedimentological and ecological evolution. *Quaternary International*, **221** (1-2), 141-158.
- SCOTT-JACKSON J. & WALKINGTON H., 2005** - Methodological issues raised by laser particle size analysis of deposits mapped as Clay-with-flints from the Palaeolithic site of Dickett's Field, Yarnhams Farm, Hampshire, UK. *Journal of Archaeological Science*, **32**, 969-980.
- SHOM, 2016** - Références altimétriques maritimes - Ports de France métropolitaine et d'outre-mer. Côtes du zéro hydrographique et niveaux caractéristiques de la marée. Service Hydrographique et Océanographique de la Marine, Brest.
- SORREL P., TESSIER B., DEMORY F., DELSINNE N. & MOUAZE D., 2009** - Evidence for millennial-scale climatic events in the sedimentary infilling of a macrotidal estuarine system, the Seine estuary (NW France). *Quaternary Science Reviews*, **28**, 499-516.
- STÉPHAN P. & GOSLIN J., 2014** - Evolution du niveau marin relatif à l'Holocène le long des côtes françaises de l'Atlantique et de la Manche : réactualisation des données par la méthode des « sea-level index points ». *Quaternaire*, **25** (4), 295-312.
- STÉPHAN P., GOSLIN J., PAILLER Y., MANCEAU R., SUANEZ S., VAN VLIET-LANOË B., HÉNAFF A. & DELACOURT C., 2015** - Holocene salt-marsh sedimentary infillings and relative sea-level changes in West Brittany (France) from foraminifera-based transfer functions. *Boreas*, **44** (1), 153-177.
- SITZIA L., BERTRAN P., BAHAIN J.-J., BATEMAN M.D., HERNANDEZ M., GARON H., DE LAFONTAINE G., MERCIER N., LEROYER C., QUEFFELEC A. & VOINCHET P., 2015** - The Quaternary coversands of southwest France. *Quaternary Science Reviews*, **124**, 84-105.
- STUIVER M. & REIMER P.J., 1993** - Extended 14C data base and revised CALIB 3.0. 14C age calibration program. *Radiocarbon*, **35**, 215-230.
- SUANEZ S., DEHOUC A. & STÉPHAN P., 2008** - Incertitude de la mesure de terrain en géomorphologie littorale. Approche statistique et quantification des marges d'erreur. In P. Allard, D. Fox & B. Picon (eds.) *Incertitude et environnement, la fin des certitudes scientifiques*. Edition EDISUD, Aix-en-Provence, 127-139.
- SUCHÝ V., SÝKOROVÁ I., HAVELCOVÁ M., MACHOVIČ V., ZEMAN A. & TREJTNAROVÁ H., 2013** - Cementation and blackening of Holocene sands by peat-derived humates: A case study from the Great Dune of Pilat, Landes des Gascogne, Southwestern France. *International Journal of Coal Geology*, **114**, 19-32.
- SWINDLES G.T., LAWSON I.T., MATTHEWS I.P., BLAAUWC M., DALEY T.J., CHARMAN D.J., PROLANDF T., PLUNKETT G., SCHETTLER G., GEAREY B.R., TURNER T.E., REA H.A., ROE H.M., AMESBURY M.J., CHAMBERS F.M., HOLMES J., MITCHELL F.J.G., BLACKFORD J., BLUNDELL A., BRANCH N., HOLMES J., LANGDON P., MCCARROLL J., McDERMOTT F., O.OKSANENK P., PRITCHARD O., STASTNEY P., STEFANINI B., YOUNG D., WHEELER J., BECKER K. & ARMIT I., 2013** - Centennial-scale climate change in Ireland during the Holocene. *Earth-Science Reviews*, **126**, 300-320.
- TASTET J.-P. & PONTEE N.I., 1998** - Morpho-chronology of coastal dunes in Médoc. A new interpretation of Holocene dunes in Southwestern France. *Geomorphology*, **25**, 93-109.
- TASTET J.-P., 1998** - Chronologie et cartographie d'un complexe dunaire côtier holocène, l'exemple aquitain du Nord-Médoc (France). *Quaternaire*, **9** (3), 157-167.
- TASTET J.-P., ROUSSOT-LARROQUE J. & CLAVÉ B., 2000A** - Palaeo-environmental Study Area P15: West Bank of the Gironde Estuary, west coast, France. In R.G. McInnes, D.J. Tomalin & J. Jakeways (dir.), *LIFE Environment Project: LIFE-97 ENV/UK/000510 1997-2000 Coastal change, climate and instability: Final Technical Report*. Isle of Wight Center for the Coastal Environment, Newport, 57 p.
- TASTET J.-P., ROUSSOT-LARROQUE J. & CLAVÉ B., 2000B** - Palaeo-environmental Study Area P16 East Bank of the Gironde Estuary, west coast, France. In R.G. McInnes, D.J. Tomalin & J. Jakeways (dir.), *LIFE Environment Project: LIFE-97 ENV/UK/000510 1997-2000 Coastal change, climate and instability: Final Technical Report*. Isle of Wight Center for the Coastal Environment, Newport, 66 p.
- TASTET J.P., 1999** - Le Pléistocène de la façade Atlantique du Nord Médoc (France) : Etat des connaissances sur la lithologie et la chronostratigraphie des « Argiles du Gurp ». *Quaternaire*, **10**, 199-212.
- TERS M., 1973** - Les variations du niveau marin depuis 10 000 ans le long du littoral atlantique français. In *Le Quaternaire : géodynamique, stratigraphie et environnement : travaux français récents*. Comité National Français de l'INQUA, Paris, 114-135.
- TESSIER B., BILLEAUD I., SORREL P., DELSINNE N. & LESUEUR P., 2012** - Infilling stratigraphy of macrotidal tide-dominated estuaries. Controlling mechanisms: Sea-level fluctuations, bedrock morphology, sediment supply and climate changes (The examples of the Seine estuary and the Mont-Saint-Michel Bay, English Channel, NW France). *Sedimentary Geology*, **279**, 62-73.
- TISDALL E.W., MCCULLOCH R.D., SANDERSON D.C.W., SIMPSON I.A. & WOODWARD N.L., 2013** - Living with sand: A record of landscape change and storminess during the Bronze and Iron Ages Orkney, Scotland. *Quaternary International*, **308-309**, 205-215.
- TISNÉRAT-LABORDE N., PATERNE M., MÉTIVIER B., ARNOLD M., YIOU P., BLAMART D. & RAYNAUD S., 2010** - Variability of the northeast Atlantic sea surface $\Delta^{14}\text{C}$ and marine reservoir age and the North Atlantic Oscillation (NAO). *Quaternary Science Reviews*, **29** (19-20), 2633-2646.
- VAN GEEL B., BUURMAN J. & WATERBOLK H.T., 1996** - Archaeological and palaeoecological indications of an abrupt climate change in the Netherlands, and evidence for climatological teleconnections around 2650 BP. *Journal of Quaternary Science*, **11**, 451-460.
- VAN VLIET-LANOË B., GOSSLIN J., HALLEGOUET B., HÉNAFF A., DELACOURT C., FERNANE A., FRANZETTI M., LE CORNEC E., LE ROY P. & PENAUD A., 2014** - Middle- to late-Holocene storminess in Brittany (NW France): Part I - morphological impact and stratigraphical record. *The Holocene*, **24** (4), 413-433.
- VERDIN F., EYNAUD F., STÉPHAN P., ARNAUD-FASSETTA G., BOSQ M., BERTRAND F., SUANEZ S., COUTELIER C., COMTE F., WAGNER S., BELINGARD C., ARD V., MANEN C., SAINT-SEVER G. & MARCHAND G., 2019** - Humans and their environment on the Médoc coastline from the Mesolithic to the Roman period. *Quaternaire*, **30**, 77-95.
- VINCENT P., 1996** - Variation in particle size distribution on the beach and windward side of a large coastal dune, southwest France. *Sedimentary Geology*, **103**, 273-280.
- VISSET L., BORNE V., MAISONNEUVE E. & NIKODIC J., 1989** - Environnement du site néolithique des Chatelliers-en-Auzay (Vendée). *Bulletin de la Société Préhistorique Française*, **86** (7), 203-205.
- VISSET L., VEOLTZEL D., MAISONNEUVE E. & NIKODIC J., MARGEREL J.-P. & BORNE V., 1990** - Paléoenvironment holocène des marais du Rocher en Maillezais dans le marais poitevin (littoral atlantique, France). *Quaternaire*, **1** (2), 111-121.
- WANG J., MASSÉ L. & TASTET J.-P., 2006** - Sedimentary facies and paleoenvironmental interpretation of a Holocene marsh in the Gironde Estuary in France. *Acta Oceanologica Sinica*, **25** (6), 52-62.
- WATT P.J. & DONOGHUE D.N.M., 2005** - Measuring forest structure with terrestrial laser scanning. *International Journal of Remote Sensing*, **26**, 1437-1446.
- ZAITLIN B.A., DALRYMPLE R.W. & BOYD R., 1994** - The stratigraphic organization of incised valley systems associated with relative sea level change. In: R.W. Dalrymple, R.J. Boyd & B.A. Zaitlin (eds.), *Incised valley systems: origin and sedimentary sequences. Special publication - Society for Sedimentary Geology*, **51**, 45-60.